UCL Université catholique de Louvain

École polytechnique de Louvain (EPL)

Separation of dimethyl carbonate and methanol mixture by pervaporation using HybSi ceramic membrane

Dissertation presented by
Antoine GOFFINET

for obtaining the master's degree in
Chemical and Materials Engineering

Supervisors
Patricia LUIS ALCONERO

Readers
Iwona CYBULSKA, Denis DOCHAIN, Wenqi LI

Academic year 2017-2018

Abstract

In the current context of high biodiesel production, some by-products are created particularly glycerol. Glycerol has a wide range of applications however its market is supersaturated as its production is very high. A solution found is the production of a value added component from glycerol. This value added component is the glycerol carbonate (GC) produced by transesterification reaction of glycerol with dimethyl carbonate (DMC). The reaction includes four components: glycerol, DMC, GC and methanol. As methanol and DMC make up an azeotropic mixture, it is not possible to separate them by distillation. Pervaporation is a solution for this separation as it can break the azeotrope mixture and have other advantages especially energy saving. The pervaporation using polymeric membrane presents disadvantages as the low thermally and chemically resistance. Therefore another kind of membrane is needed. As ceramic membrane resistance is higher, the commercial HybSi ceramic is selected for this thesis experiments. This study aim to analyse the separation of DMC and methanol by pervaporation. The separation performance of HybSi membrane is evaluated at 40-50-60°C with binary mixture of different concentrations. The permeation through the membrane is analysed by the solution-diffusion model.

The results showed low permeate flux between 0 and 0.86 $\left[\frac{kg}{hm^2}\right]$. The separation factor is approximately equal to 1 demonstrating low separation efficiency. Temperature and feed concentration influence the performance results. The major drawback of this membrane is the performance results instability.

This work shows that HybSi membrane is not suitable for separation of DMC and methanol by pervaporation.

Acknowledgments

I would like to express my gratitude to advisor Patricia Luis Alconero who supported my work with patient guidance, encouragement and constructive suggestions. I am thankful for the interest she gave me through her courses and this project.

My research would have been impossible without the presence of my assistant Wenqi Li for his continuous support and useful remarks but also the help in overcoming numerous obstacles I have been facing through my research especially with the membrane which was not as expected.

I would like to thank KIMA department (chemical and materials engineering department) for giving me the opportunities to use high-performance equipment.

My sincere thanks also go to Luc Wautier and Frédéric Van Wonterghem, laboratory managers. They always paid attention to the correct functioning of my experiments and ensured my security through utilization of laboratory devices.

I would like to express my thanks to both readers Iwona Cybulska and Denis Dochain who have taken time to be interested in my study.

Thanks also to Cristhian Molina Fernández sharing laboratory equipment with a good cooperation.

Last but not least, I would like to thank my family and friends supporting me throughout all my studies and the writing of this work.

Contents

List of Tables

List of Figures

Nomenclature

α	Selectivity,	$[-]$
β	Separation factor,	$[-]$
$\frac{P_i}{l}$	Permeance of component i,	$\left[1GPU = 10^{-6}\frac{cm^3}{cm^2 \cdot s \cdot cmHg}\right]$
$\frac{P_{i,\infty}}{l}$	Pre-exponential factor for Arrhenius equation,	$[GPU]$
γ_i	Activity coefficient,	$[-]$
D_i	Diffusion coefficient,	$\left[\frac{m^2}{s}\right]$
E_a	Activation energy,	$\left[\frac{J}{mol}\right]$
J_i	Permeate flux of component i,	$\left[\frac{kg}{h \cdot m^2}\right]$
j_i	Molar flux for component i,	$\left[\frac{L}{h \cdot m^2}\right] = \left[\frac{m^3}{h \cdot m^2}\right]$
l_M	Membrane thickness,	$[m]$
m_i	Molecular weight of component i,	$\left[\frac{g}{mol_i}\right]$
m_t	Molecular weight of the mixture,	$\left[\frac{g}{mol}\right]$
N_i	Molar flux of component i,	$\left[\frac{mol_i}{s \cdot m^2}\right]$
P_i^0	Vapour pressure of component i,	$[atm]$
P_p	Permeate pressure,	$[atm]$
T	Temperature,	$[°C]$
v_i^G	Molar volume of gas i,	$\left[\frac{L}{mol_i}\right]$
x_i	Mole fraction of component i in the feed,	[-]
y_i	Mole fraction of component i in the permeate,	[-]
A	Effective membrane surface area,	$[m^2]$

APTEOS	3-aminopropyl-triethoxysilane,	[-]
CS	Chitosan–silica hybrid,	[-]
DEG	Diethylene Glycol,	[-]
DMC	Dimethyl carbonate,	[-]
GC	Glycerol carbonate,	[-]
HybSi	Hybrid Silica,	[-]
J	Permeate total flux,	$\left[\frac{kg}{h \cdot m^2}\right]$
MeOH	Methanol,	[-]
PDMS	Polydimethylsiloxane,	[-]
PTMSP	Poly[(trimethylsilyl)propyne],	[-]
PVDF	Polyvinylidene fluoride,	[-]
STA	Silicotungstic acid hydrate,	[-]
t	Time,	$[h]$
VLE	Vapour liquid equilibrium,	[-]
VOC	Volatile organic compound,	[-]
w	Weight,	$[kg]$

Chapter 1

Introduction

In this chapter, literature study has been done. First of all the context of this thesis will be discussed. After finding which compound has to be separated, the method in order to separate them is selected. A comparison of different membranes used nowadays is done and ceramic membrane (HybSi membrane) is chosen. Finally the objectives of the this thesis will be stated.

1.1 Context: Biodiesel production

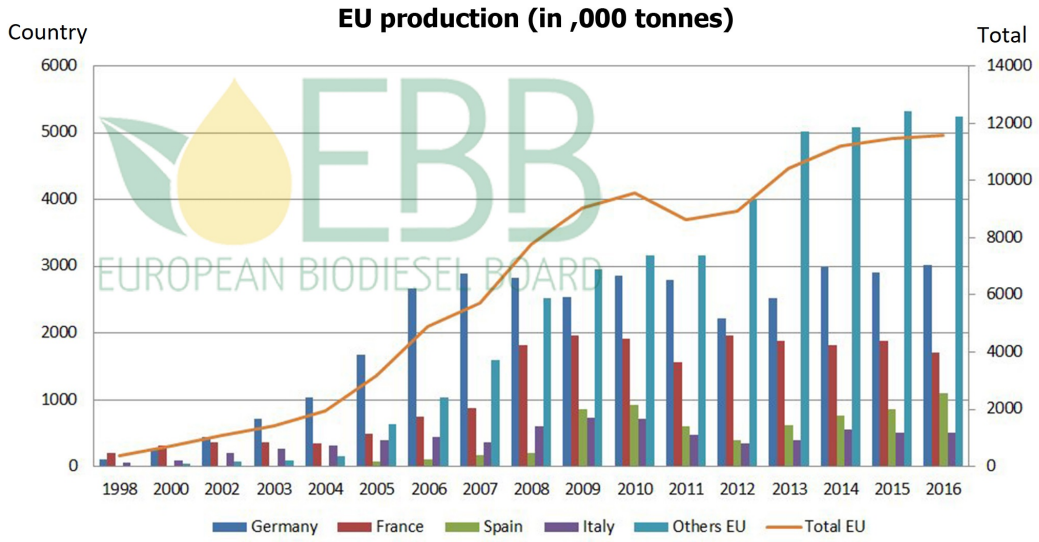

Figure 1.1: Evolution of biodiesel production in Europe [1].

As illustrated on Figure 1.1, it can be observed that the biodiesel production increases nowadays due to high diesel need especially in Europe and the evolution of biofuel in the modern-day society. Nevertheless the main drawback of biodiesel is the price.

Biodiesel can be derived from different oils mainly composed of triglycerids. The transformation reaction to form biodiesel is called transesterification as exposed on the Figure 1.2. Alcohol (usually methanol) and ester react in order to make some fatty acid also called ester fatty acid. But this reaction is quite slow, a catalyst is frequently added. It was noted that the production of every 10 kg of biodiesel via the transesterification process yields approximately 1 kg of crude glycerol which is a by-product [31].

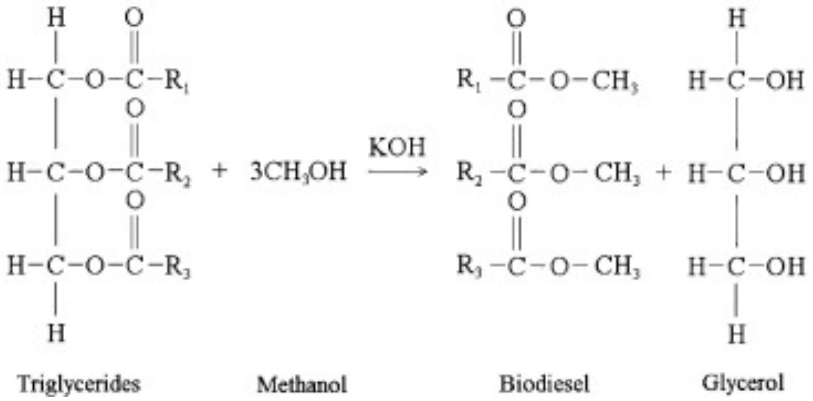

Figure 1.2: Biodiesel production.

Glycerol is a valuable by-product as it has a wide range of industrial applications [31]. At present, glycerol has over two thousand different applications, especially in pharmaceuticals and drugs (giving pills humidity and increasing liquid drugs viscosity, plasticizers for medicine capsules), personal care (cough syrups, ear infection medicines, toothpastes to prevent hardening and drying out in the tube), foods and beverage (sweetener and preservative agent for extracts of tea for example), cosmetics, excellent solvent for different chemicals, as shown in Figure 1.3. Glycerol is a nontoxic, edible, biodegradable compound so it is very advantageous for these environmental features.

.

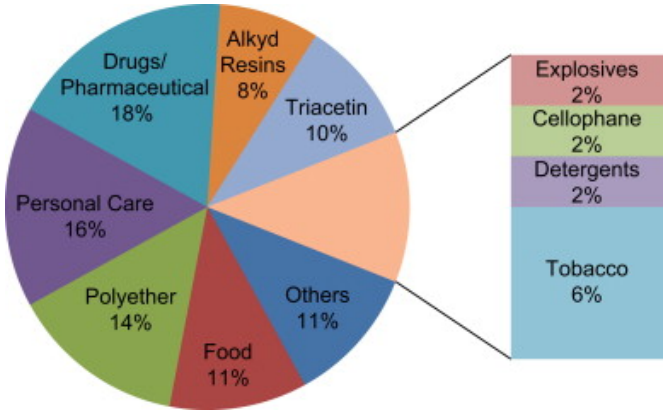

Figure 1.3: Glycerol applications [31].

It was reported that present glycerol market is low due to its abundance caused by high biodiesel production. Then researches are done now to find valuable compounds produced from glycerol.

1.2 Glycerol carbonate

Glycerol carbonate (GC) is one of the glycerol derivatives that attracts scientific and industrial interests due to its low toxicity, low flammability, biodegradability, high boiling point, slight viscosity and water solubility [37] [30]. It is a high value-added product with market price greater than 8141 US$/ton [32].

GC has found applications as a high boiling polar solvent, an intermediate in organic synthesis and as bio-chemical-monomer precursor for the synthesis of polycarbonates, polyurethanes, glycidol-based polymers and surfactants, emulsifier in cosmetics and in cleaning agent [30] [2], in paints, gas separation membrane [37].

The potential industrial uses of GC are presented in Figure 1.4 [32].

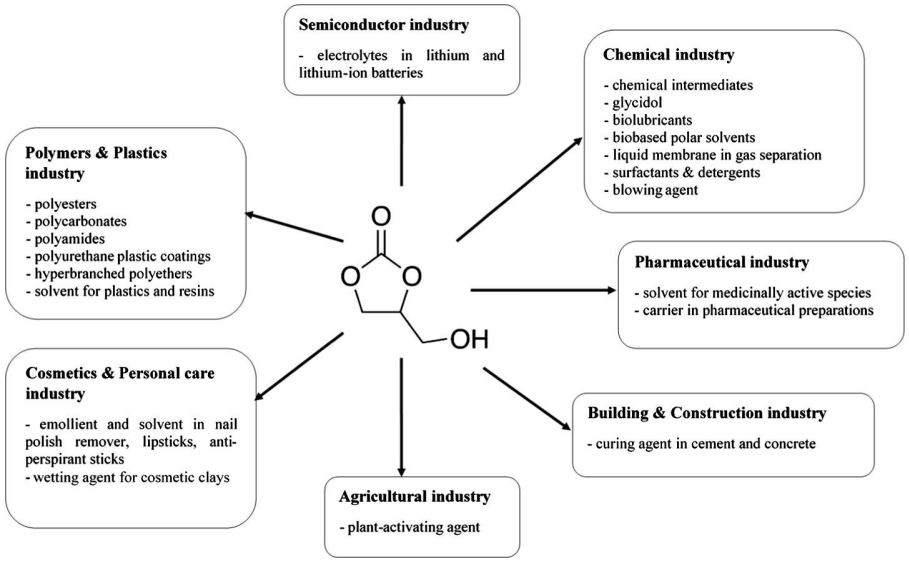

Figure 1.4: Glycerol carbonate applications [32].

1.2.1 Glycerol carbonate production

GC can be produced by different processes from glycerol as glycerol phosphogenation (limited due to the toxicity of phosgene) or glycerol direct carboxylation/carbonation with CO2 (limited by thermodynamics); oxidative carbonylation of glycerol with CO and Oxygen; transesterification of glycerol with ethylene carbonate or dimethyl carbonate . GC could also be produced by glycerolyse with urea [37] [2].

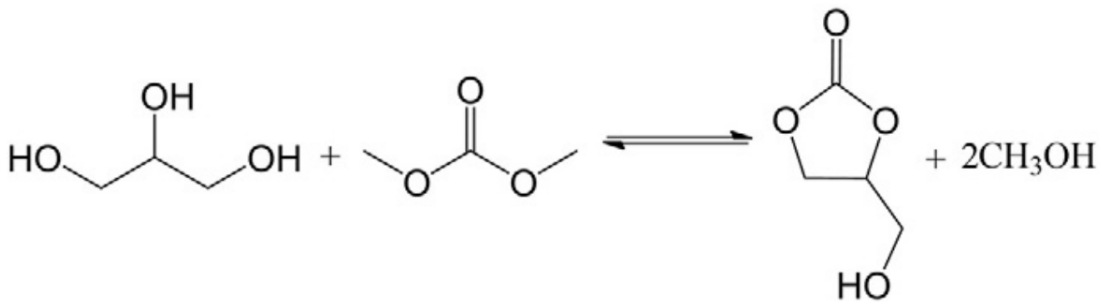

Figure 1.5: Transesterification reaction to produce glycerol carbonate.

The transesterification reaction is shown in Figure 1.5. This is an equilibrium reaction then the conversion is not very high. Some parameters can be modified in order to increase the conversion such as temperature, molar ratio of DMC to glycerol, time and catalyst (choice and quantity, heterogeneous or homogeneous).

A lot of catalysts can be used [32]:

- Homogeneous: K_2CO_3, KOH, NaOH, Ionic liquid or H_2SO_4
- Heterogeneous: CaO, $CaCO_3$, Na_2O, ZnO, MgO, etc

The optimal conditions for transesterification reaction are (using Na_2SiO_3 – 200 catalyst[1])[37]: a ratio DMC to glycerol of 4:1, 75°C, 5 %wt catalyst and during 2.5 hours.

With this conditions the glycerol carbonate conversion reaches 97.8 % and the yield equal to 95.5 % [37].

[1] Na_2SiO_3 – 200 has been calcined at 200°C. This catalyst is stable, non toxic, cheap, has a high activity and easiness of re-usability.

1.3 Azeotrope mixture methanol-dimethyl carbonate

As said before, an equilibrium mixture is made up four compounds: dimethyl carbonate, glycerol, methanol and glycerol carbonate. However the separation of these four compounds is very difficult to achieve. Separation of dimethyl carbonate (DMC) with methanol (MeOH) is fundamentally difficult as DMC forms an azeotrope with MeOH at 86.47 %mol at 1 bar of MeOH as shown on Figure 1.6. The computation of this curve is explained in ***Appendices*** Section 5.1.3. Consequently common distillation can not be used. Indeed, in a distillation column the azeotrope mixture will be obtained at the bottom or upper flow depending on the feed concentration. A computation example of stages number for distillation column can be found in ***Appendices*** Section 5.2. Even if few distillation columns are put in series, a good separation is unfeasible.

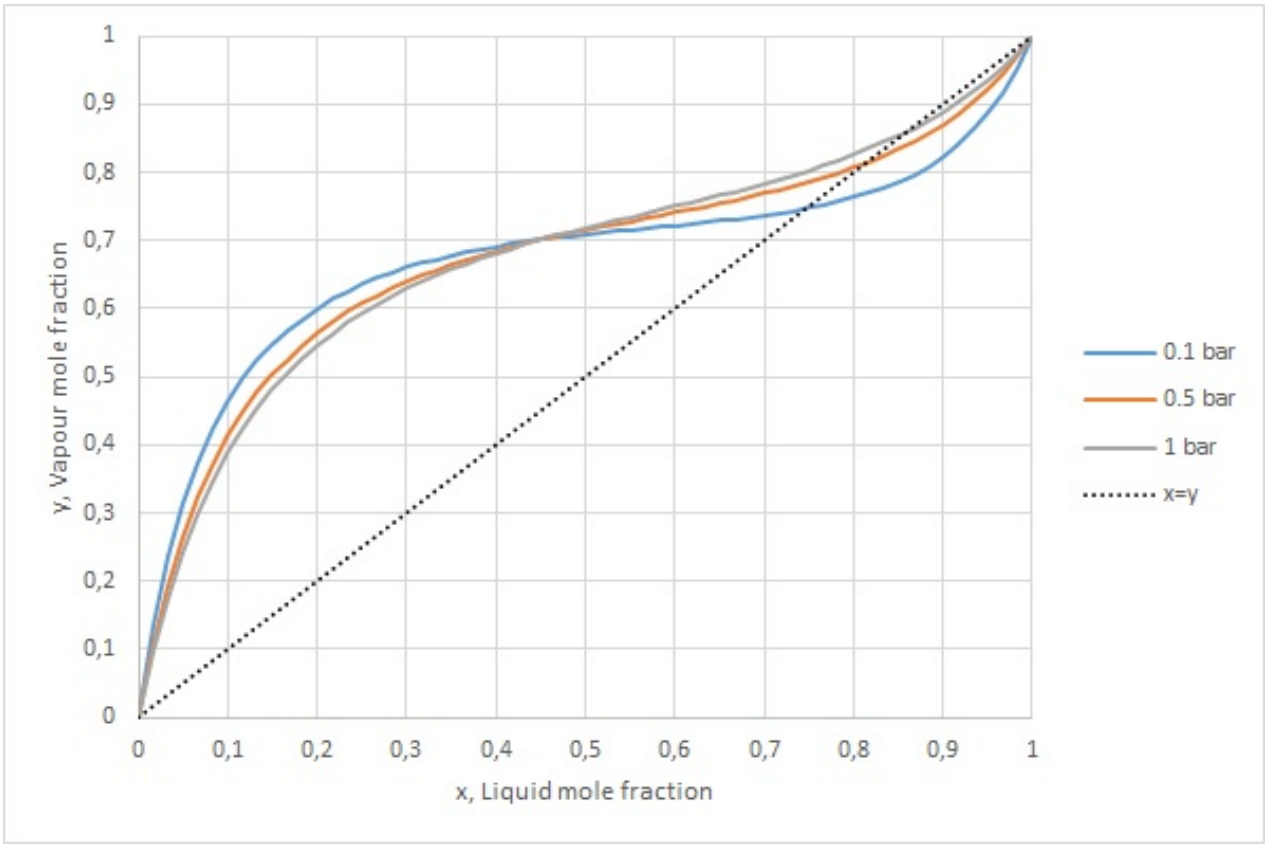

Figure 1.6: Azeotrope mixture of methanol and dimethyl carbonate.

There are different distillation techniques frequently used to break the azeotrope: Pressure-swing distillation, azeotopic distillation, and extractive distillation. Extractive and azeotropic distillation require the addition of mass separating agent or so-called entrainer or simply solvent as well as phenol (organic solvent) and others as ionic liquids [15] [5].

Pressure-swing distillation is a technique using the variation of the azeotrope point with the pressure as illustrated on Figure 1.6. As it can be observed, significant variations of the azeotropic point need high variations in pressure which is fundamentally difficult and expensive to set up.

Extractive distillation can be observed on Figure 1.7 with Ethyl benzoate as solvent but other compounds can also be used as solvent (Methyl salicylate, Phenol, Dimethyl oxalate, 2-Ethoxyethanol or 4-Methyl-2-pentanone). The principle of extractive distillation is quite simple, due to the presence of the solvent, methanol can be separated in the first column than DMC is separated from the solvent in the second column and solvent is eventually recycled.

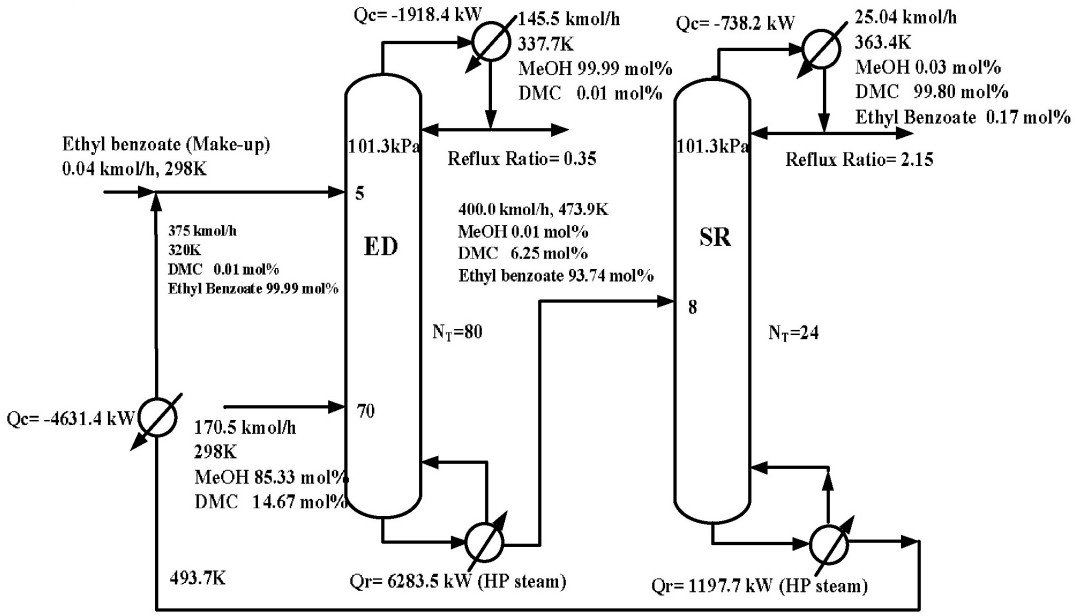

Figure 1.7: Advanced distillation example - Extractive distillation [15].

Two major drawbacks of this method are high energy consumption and solvent usage.

1.4 Methanol - dimethyl carbonate: separation by pervaporation using polymeric membrane

DMC and methanol separation through distillation is very complicated as shown earlier. Then pervaporation is a good alternative as it is economical, energy-saving, and eco-friendly and flexible[18] [25].

Pervaporation is already used in the industry for some applications like dehydration of organic solvents, separation of dissolved organics from water and separation of organic liquid mixtures [24].

A basic example of industrial application is dehydration from ethanol. Ethanol and water mixture make up an azeotrope which is not possible to distillate. This is the reason why hybrid system combining pervaporation and distillation has been developed.

1.4.1 Basic principle of pervaporation

The term pervaporation means permselective and evaporation. This technique allows separating compounds from liquid mixture using a dense membrane. The pervaporation does not separate the compounds by thermal equilibrium as distillation but by kinetics. This way components of azeotropic mixture can be separated. As Figure 1.8 shows, a compound (A on the figure) permeates fast through the membrane while other slowly, that is the way the separation occurs. Due to the vacuum applied at permeate side, the liquid evaporates somewhere in the membrane.

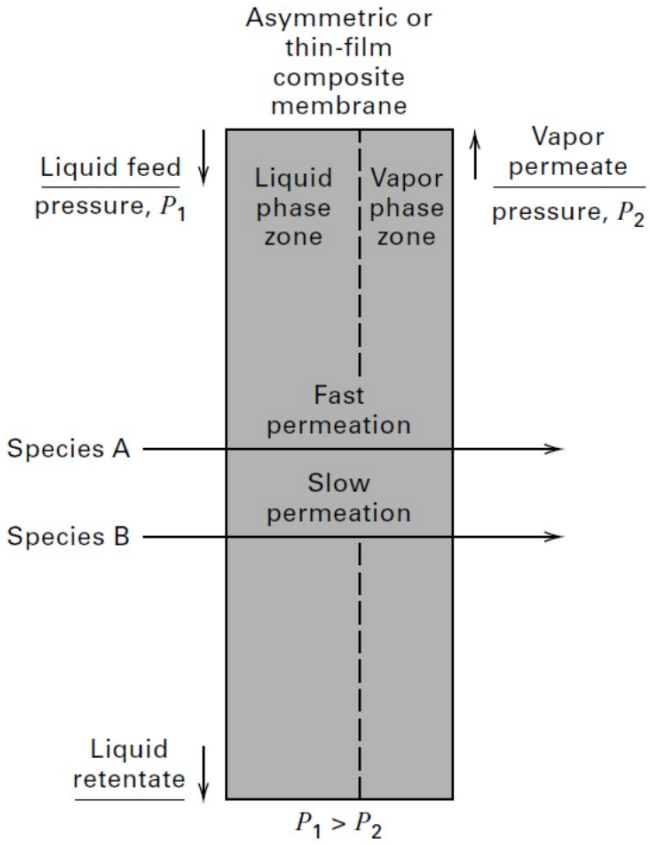

Figure 1.8: Pervaporation principle [6].

On Figure 1.9, the usual flow-sheet of a pervaporation installation is shown. The feed is divided in two parts. One part, the retentate, does not pass through the membrane and which is recycled. A second part, the permeate, passes through the membrane. The permeate is condensed in order to have liquid solution.

The major advantage of this configuration is the possible increase of the reaction yield. Due to the membrane selectivity towards one product, this one is removed from the mixture then the yield is improved due to Le Chatelier principle. This major pervaporation advantage described above is only possible if the reactor is combined with the separation media nevertheless this point is outside of this document scope.

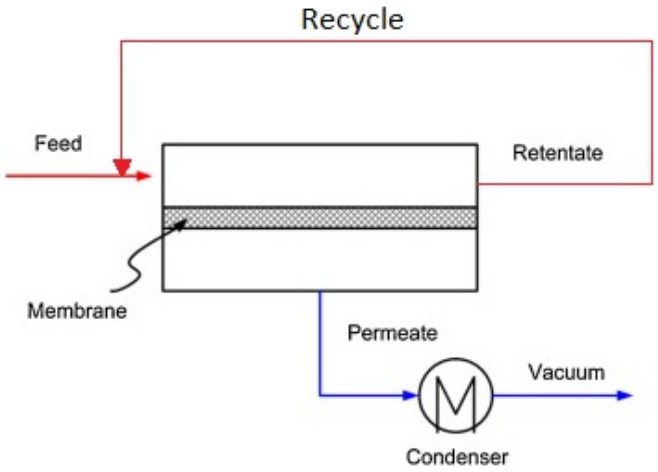

Figure 1.9: Pervporation functioning [28].

The mass transfer mechanism of pervaporation is usually described by the solution diffusion model as shown on Figure 1.9. There are three major steps of permeation through the membrane, first sorption then diffusion through the membrane and finally desorption (which is very fast due to the vacuum).

The solution diffusion model is explained later in the Section 2.2.2.

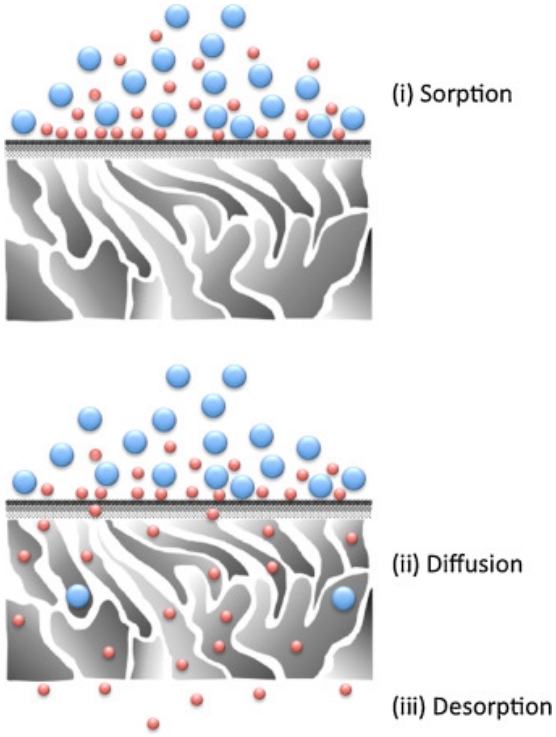

Figure 1.10: Graphical representation of the solution diffusion mechanism [28].

A numerical case study compares the difference between processes for the production of acetal [16]. The three cases are: basic one (tubular reactor and distillation), reactive distillation and hybrid process combining reactor and pervaporation (Hybsi membrane). The comparison is shown on Table 1.1. This data confirms all the advantages previously stated.

Table 1.1: Processes comparison [16].

	Basic case	Reactive distillation	Pervaporaton
Conversion (Plug flow)	39%	41%	43%
Steam 3.5bar ($\frac{kg_{steam}}{kg_{acetal}}$)	1.80	3.76	1.12
Cooling water ($\frac{kg_{H_2O}}{kg_{acetal}}$)	33.68	78.20	19.51
Electricity ($\frac{KWh}{kg_{acetal}}$)	0	0	0.09

Other articles [3] [12] also confirm that pervaporation (using Hybsi ceramic membrane, also used for this thesis) allows an energy saving up to 50%.

1.4.2 Pervaporation using polymeric membrane

One of the most known pervaporation applications is for ethanol/water separation. There are a lot of studies about this. Indeed with the evolution of bioethanol market, its production has been increased. Nevertheless biethanol contains water which must be removed because water decreases the fuel efficiency. As ethanol makes an azeotrope mixture with water, pervaporation technology has been chosen to dehydrate bioethanol. More information and result examples can be found in the literature [38].

Pervaporation of methanol and DMC using polymeric membrane

From different studies found in literature, temperature and concentration have strong impact on the membrane separation performance, the goal of pervaporation is to obtain high flux and high separation factor in order to have an efficient separation.

Some results for DMC/MeOH separation using polymeric membrane have been found in the literature and are displayed on Table 1.2.

The first class and the most frequent membrane is PDMS membrane. Chitosan silica hybrid (CS) membrane is the second class. This membrane type is hydrophilic. Another type of membrane is Nafion®.

Table 1.2: Results for DMC-Methanol separation through pervaporation using polymeric membrane.

Membrane	Temperature [$°C$]	Composition [$MeOH$]	Separation factor	Flux [$\frac{kg}{m^2h}$]	Reference
PDMS					
PDMS/PVDF composite	40	72 %wt	3.95	0.4872	[42]
Hydrophibic nano-silica/PDMS	40	70 %wt	3.94	0.702	[36]
CS					
STA/CS	50	10 %wt	67.3	1.163	[10]
STA/CS	50	70 %wt	33	1.48	[10]
STA/CS	40	10 %wt	90	1.03	[10]
CS	50	10 %wt	21	0.21	[10]
CS	50	70 %wt	12	0.32	[10]

Membrane	Temperature [$°C$]	Composition [$MeOH$]	Separation factor	Flux [$\frac{kg}{m^2h}$]	Reference
Crosslinked chitosan by dilute sulfuric acid	35	70 %wt	66	0.23	[40]
Crosslinked chitosan by dilute sulfuric acid	45	70 %wt	60	0.26	[40]
Crosslinked chitosan by dilute sulfuric acid	35	10 %wt	50	0.06	[40]
Crosslinked chitosan by dilute sulfuric acid	45	10 %wt	40	0.1	[40]
Crosslinked chitosan by dilute sulfuric acid	35	70 %wt	10	0.12	[39]
Crosslinked chitosan by dilute sulfuric acid	45	70 %wt	10	0.18	[39]
Crosslinked chitosan by dilute sulfuric acid	35	11 %wt	35	0.040	[39]
Crosslinked chitosan by dilute sulfuric acid	45	10 %wt	34	0.048	[39]
CS	40	30%wt	22	0.22	[9]
CS	50	30%wt	16.6	0.26	[9]
Chitosan crosslinked with APTEOS	40	30%wt	45.3	1.05	[9]
Chitosan crosslinked with APTEOS	50	30%wt	41.4	1.158	[9]
Chitosan crosslinked with APTEOS	50	70 %wt	30.1	1.265	[9]
Nafion®					
	40	78%mol	2	4	[20]
	40	13%mol	19	0.8	[20]

For PDMS membrane [36], increasing MeOH content increases separation factor but decreases flux. Raising the temperature increases flux while decreases separation factor.

For CS membrane, generally increasing MeOH content increases the flux but decreases the separation factor. As for PDMS membrane, raising the temperature increases flux while decreases separation factor. Finally crosslinking helps having an improved separation as the flux and the separation factor is higher.

1.5 Advantage of ceramic membrane

Pervaporation performance is mainly determined by the membrane. Hence the membrane material is crucial for separation. Nowadays polymeric membrane is widely used due to its low price and fabrication ease. Nevertheless chemical, mechanical and thermal resistance are the major problems of polymeric membrane and the lifetime of these membranes is short.

Ceramic membrane is the solution to these problems as the membrane has high mechanical, thermal and chemical resistance, non swelling behaviour, easy cleaning [22]. Hence ceramic membrane type is the main subject of a wide range of research currently. It is used for ultrafiltration, nanofiltration, reverse osmosis, gas separation and pervaporation [22].

Ceramic membranes are a kind of artificial membrane made from inorganic materials such as alumina, titania, zirconia oxides, silicon carbide or some glassy materials. The drawbacks of ceramic membrane are the price, complex processing and the low membrane surface area per volume [33].

This kind of membrane also shows high fluxes and separation factor for pervaporation [34] as shown in Section 1.6. That is why the performance of ceramic membrane will be the content of this study.

Membrane is usually composed of a porous inorganic support and a selective layer. The selective layer applied on the support determines the membrane resistance to different medium conditions [4]. This type of membrane processes higher permeation flux and stability simultaneously, for this reason ceramic membrane is suitable for industrial application [18].

Composite membrane also demonstrates an interesting behaviour. As shown on Figure 1.11, the combination of ceramic support and polymeric selective layer allows having better properties as high mechanical and thermal resistance leading to high performance pervaporation [18] [24]. This membrane type is being the focus of some studies. It could be used for several applications as bio-fuel recovery from fermentation broth, desulfurization of gasoline and dehydration of alcohols and esters [18] [24].

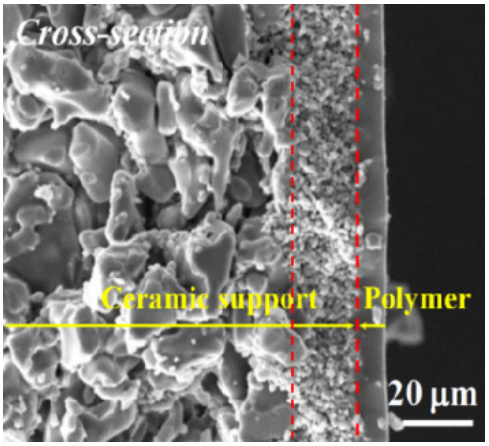

Figure 1.11: Polymer ceramic composite membrane: Ceramic support and thin layer of polymer[18].

Ceramic membrane composed of oxides has hydroxyl (OH) groups on its surface is consequently hydrophilic. Therefore, in some cases a membrane surface hydrophobization process is needed as exposed on Figure 1.12.

In several articles [22], hydrophobization process on titania, zirconia and alumina ceramic membrane were efficiently done. A very important application of this membrane is VOC removal from water. Indeed, as the VOC legislation has been changed, the industry has to adapt which makes pervaporation using hydrophobized ceramic membrane an appropriate alternative. The hydrophobization is very important in this application to prevent water passing through the membrane while only the VOC pass through.

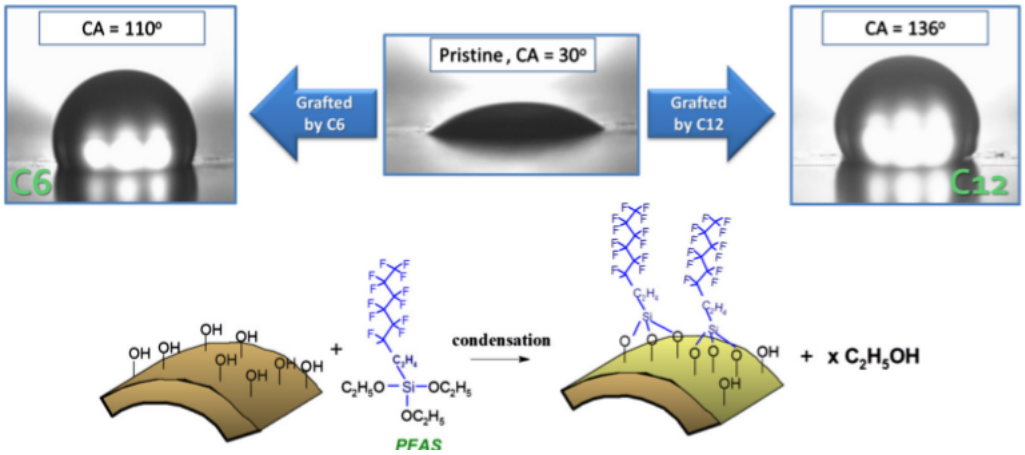

Figure 1.12: Hydrophobization process by different grafting (C6 or C12) [22].

Pervaporation efficiency is impacted by membrane material, pore size and grafting conditions (hydrophobization).

1.6 Pervaporation example using ceramic membrane

In this section, ceramic membrane used for pervaporation will be studied especially Hybsi membrane (Hybrid Silica). Ceramic membranes are at research stage but some examples can be found in literature.

Table 1.3: Results for some ceramic membrane applications.

Membrane	Mixture Composition	Temperature $[°C]$	Separation factor	Flux $[\frac{kg}{m^2h}]$	Reference
Porous silica with surface treatment	DMC-MeOH				
$SiO_2 - ZrO_2$ treatment	47-53 (%mol)	50	10	0.1	[34]
SiO_2 treatment	50-50 (%mol)	50	10-160	0.1-20	[34]
HybSi					
	Ethanol 95%wt Water 5%wt	80	120	1.5	[19]
	Isopropanol 95%wt Water 5%wt	80	10000	3.38	[19]
	DEG 99%wt water 1%wt	80	9800	0.070	[29]
	Glycerol 15%wt water 85%wt	65		10	[27]
	Glycerol 30%wt water 70%wt	65		9	[27]
	Glycerol 60%wt water 40%wt	65		3	[27]
	Glycerol 90%wt water 10%wt	65		0	[27]
	NH_3 0.1%wt water 99.9%wt	70	0.01-2.74	3.36-5.97	[41]
Hydrophobic Hybsi					
	Butanol 2%wt water 98%wt	60	15	0.5-0.6	[13]
	Butanol 2%wt water 98%wt	90	15	1.2-1.5	[13]

In the Table 1.3, results of different researches using ceramic membrane are provided.

The first type of membrane is porous silica membrane with different pore size and surface treatment (influencing the flux and separation factor). It is used in this case for DMC-MeOH separation [34]. Thus it is very interesting because the results obtained from this study can be compared with the results of this study. Several surface treatments are applied using SiO_2, SiO_2-ZzO_2. SiO_2-ZrO_2 membranes expose a separation factor <10 while the SiO_2 porous membranes had higher separation factor from 10–160. These results can be understood this way, MeOH is more hydrophilic and has lower molecule size (0.38nm) compared to DMC then the membrane must have small pores and be hydrophilic. This way, higher flux and separation factor can be achieved. For example SiO_2 has smaller pores (pore size can be adjusted) and is more hydrophilic [34].

The second ceramic membrane type is the HybSi membrane. Hybsi membrane material can be different/modified. Indeed the selective layer may be modified depending on the application. However information is not frequently available then this data should be considered carefully. This membrane is often used for dehydratation (of ethanol, isopropanol and Diethylene glycol) as it is hydrophilic [19] [4]. This is also the membrane used in this experiment study then more information about this membrane can be found in the Section 2.1.1. Another application for Hybsi membrane is gas separation as for $H_2, He, CO_2, N_2, C_3H_8$ [21].

The third case is different, the hybrid silica membrane has been hydrophobized in order to let passing butanol trough the membrane [13].

1.7 Objectives

Now that this study context has been set. Two components (methanol and dimethyl carbonate) must be separated through pervaporation. Several membranes have been already used for this separation. As these membranes do not satisfy on a chemically and thermal resistance view point, another kind of membrane must be tested. As ceramic membrane is stabler, HybSi ceramic membrane has been chosen. Its performance of pervaporation separation process will be verified and this is the main goal of this study.

First of all, the experimental conditions and the model to analyse results will be explained in the materials and methods chapter. Afterwards experimental results of this study will be provided and discussed. Finally, the conclusion on this membrane performance will be described.

Chapter 2

Materials and methods

2.1 Materials

2.1.1 Membrane

The membrane selected is an HybSi ceramic membrane supplied by Pervatech Netherlands [8]. The membrane choice has been motivated by the ceramic membrane advantages described in Section 1.5 and by the benefits of the HybSi membrane explained below. As it is a commercial membrane, the supplier does not forward all the information, consequently literature study has been done in order to know more about it.

1-Channel Hybrid Silica Membrane [7] is the membrane used. Here is these specifications: 250 x 10 mm (L x D), effective area 0,005 m^2. This membrane is just used for testing nowadays. The pore size lies between 0.3 and 0.5nm.

The substrate material is $\alpha - Al_2O_3$ while the selective layer is not known[1] (the coating is inside the tube) [8].

This membrane is a promising solution due to its high stability, indeed a pervaporation test has been done during 3 years at 150°C [4].

This membrane has various properties as hydrophilicity, porosity (0.3-0.5 nm), high temperature resistance (150°C) and can undergo a wide range of acidity ($0.5 < pH < 8.5$) [8].

The main advantages of the hydrophilic [2] Hybrid Silica membranes are quoted by PERVATECH: "energy saving, azeotropic separation, decreasing usage of cooling water, enhanced product quality also through milder conditions, reduced formation of side products, higher plant availability and chemical resistance especially for HybSi membrane and stable up to high temperatures" [8].

[1] The supplier does not tell the selective layer material for confidentiality reason.
[2] Hydrophillic means that the water content in the feed passes preferentially through the membrane.

HybSi membranes can be used for different applications [7]:

- Breaking of azeotrope
- Dehydration of organics like Alcohols, A-protic solvents, DmAc, DMSO, DMF, ethyl acetate, NMP, Phenol, THF, AcN
- In situ dehydration of condensation reactions
- Dehydration of essential oils
- Separation of low molecular weight from higher molecular weight solvents (purification)

Some researches also show this membrane application for regeneration of diethylene glycol at Russian complex gas treatment plants [19] [29] .

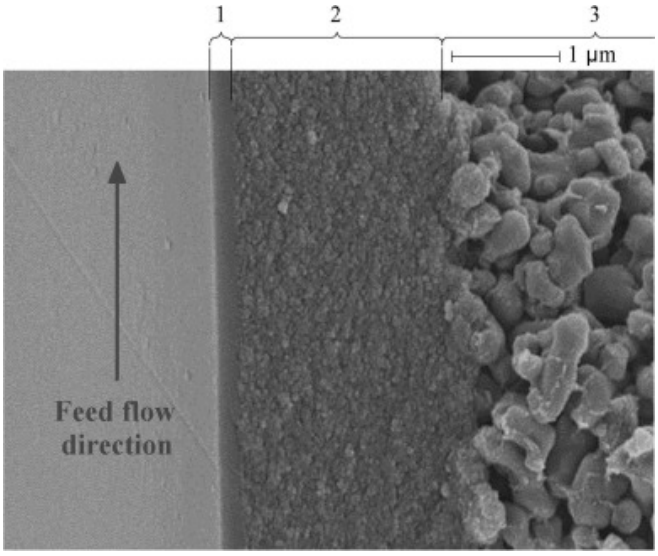

Figure 2.1: HybSi membrane [29].

Figure 2.1 shows the HybSi ceramic membrane for regeneration of diethylene glycol [29]. The different layers of the membrane can be observed. First of all the selective layer has a thickness≃200nm, for this layer the pore size is smaller than 1nm, the composition of this layer is unknown. Then the intermediate layer made of amorphous silica of thickness≃2000nm (the pore size≃4nm). The third part of the membrane is the ceramic support [29].

HybSi is an organic-inorganic hybrid material (with an inorganic base). Silicon atoms are connected to oxygen atoms in order to make siloxane group ($Si-O-Si$). However silicon is also connected to carbon atoms coming from the addition of $(CH_2)_n$ groups inside the

membrane. As shown on Figure 2.2, different groups are formed in the membrane ($Si-O-Si$ inorganic and $Si-(CH_2)_n-Si$ organic) then organic fragments are sewed into the amorphous silica spatial structure [29]. Some parameters are influenced by the inorganic part of the membrane as hydrophilicity and mechanical strength. While membrane organic part gives the hydrothermal stability and the increasing viscosity [29].

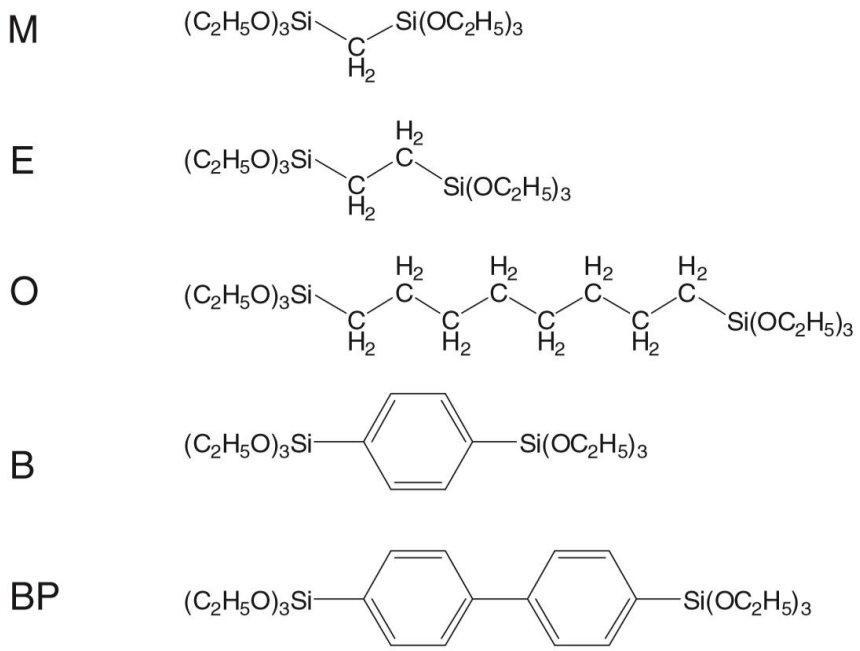

Figure 2.2: Possible bridging groups for HybSi membrane [14].

It is relevant stating that the important part is the selective layer, this is the major point for selection and separation. Thus pervaporation through ceramic support and amorphous silica intermediate layer (large pores) can generally be neglected [19].

2.1.2 Chemicals

Binary mixtures are used with different concentrations of MeOH and DMC. First experiment was done with pure compound then with different concentrations (10-30-50-70-90 %mol of MeOH).

2.1.3 Instruments

The devices are installed as shown on Figure 2.3. The pilot has several parts: a condenser (bath of isopropanol at around -40°C), a temperature sensor and a pressure sensor for the permeate side and for the feed side, a heater to heat up the mixture to the right temperature, a pump for the vacuum applied on the permeate side, a pump in order to make the fluid circulation, the membrane, the tank (maximum 1.5L and 16 bar maximum) and some pipes and valves.

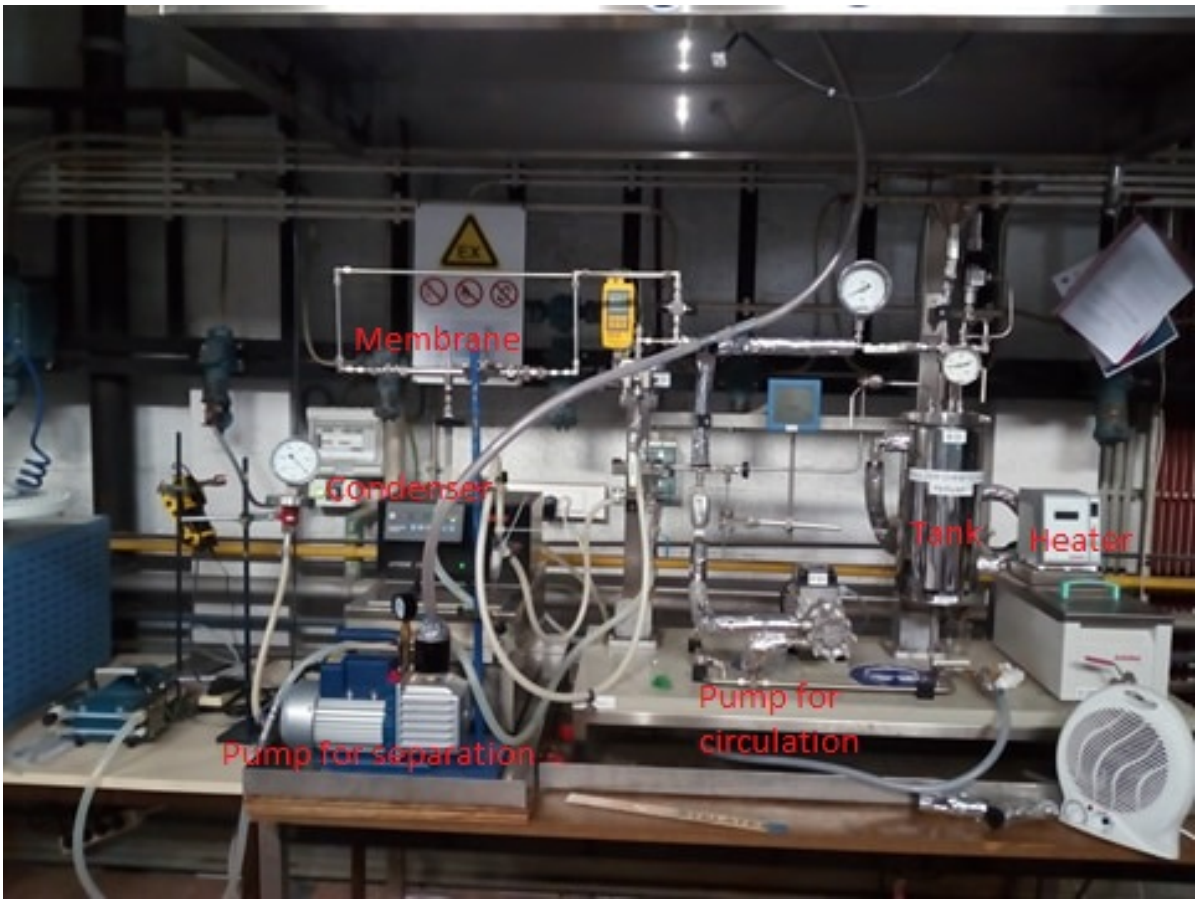

Figure 2.3: Pilot used for the experiments.

Gas chromatography

The gas chromatography used for the experiment is shown on Figure 2.4. This device analyses the different samples in order to determine the components concentration for permeate and feed side.

Figure 2.4: Gas chromatography used for the experiments.

Remark

One point remains critical: Does all the vapour condense ? Does the vapour escape from the condenser due to the vacuum ?

In order to confirm this point, a U-shaped glass has been connected in series after the main glass where condensation must occur.

The conclusion of this experiment is that there is nothing in the U-shaped glass then all the vapour phase in the permeate side were condensed as liquid phase. On the other hand, the temperature applied in the condenser allow having condensation of MeOH and MDC.

2.2 Methods

2.2.1 Experimental method

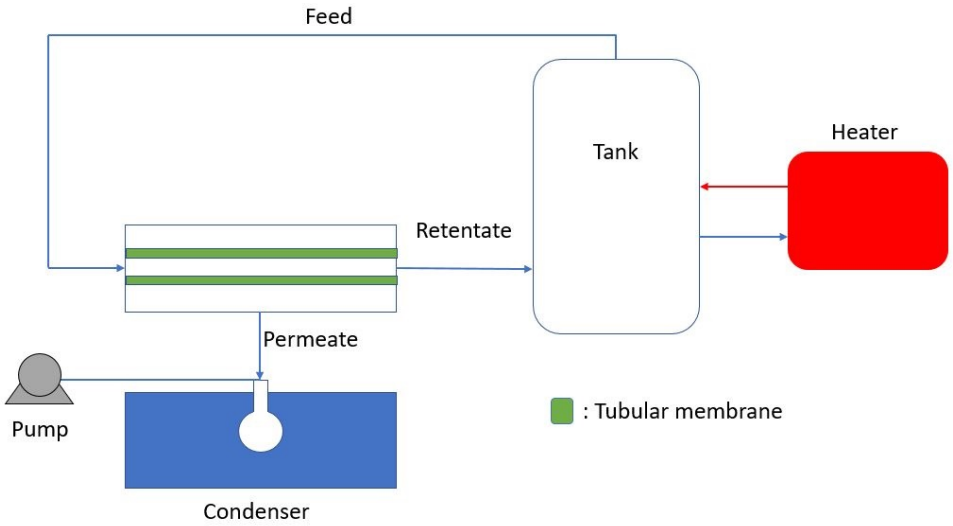

Figure 2.5: Experimental device scheme.

Figure 2.5 shows the experimental scheme as illustrated also on Figure 2.3. It can be seen that the membrane is tubular and its configuration is cross flow[3]. The permeate side is connected to a pump in order to have vacuum at this side of the membrane and there is a pump for the fluid circulation (not represented here). Table 2.1 exposes the experimental conditions.

Property	Experimental condition	Units
Permeate pressure	1	[mbar]
Condenser temperature	-40	[°C]
Feed flow	100	$\left[\frac{L}{h}\right]$
Feed pressure	1	[bar]
Experiment duration	4	[h]

Table 2.1: Experimental conditions.

The feed pressure varies with temperature. This variations (~0.4 bar) are not significant thus the pressure is assumed to be equal to 1 bar.

[3]The flow is applied tangentially across the membrane surface

Temperature (40-50-60°C) and MeOH mole fraction (0-10-30-50-70-90-100 %mol MeOH) are the parameters analysed in this document.

2.2.2 Solution-Diffusion model

Theory

This model divides the component crossing through the membrane in few stages[4]. First of all, components are transferred from retentate flow core to the membrane boundary by convection or turbulence. The second step is the components sorption by membrane surface. Thirdly the components diffuse through the membrane then the desorption into the permeate side and the final step is the transfer towards the permeate flow (this step can be neglected due to the vacuum applied on the permeate side) [19]. Those five steps are illustrated on Figure 2.6. The steps 1 and 5 are not crucial and can be skiped for the next analysis.

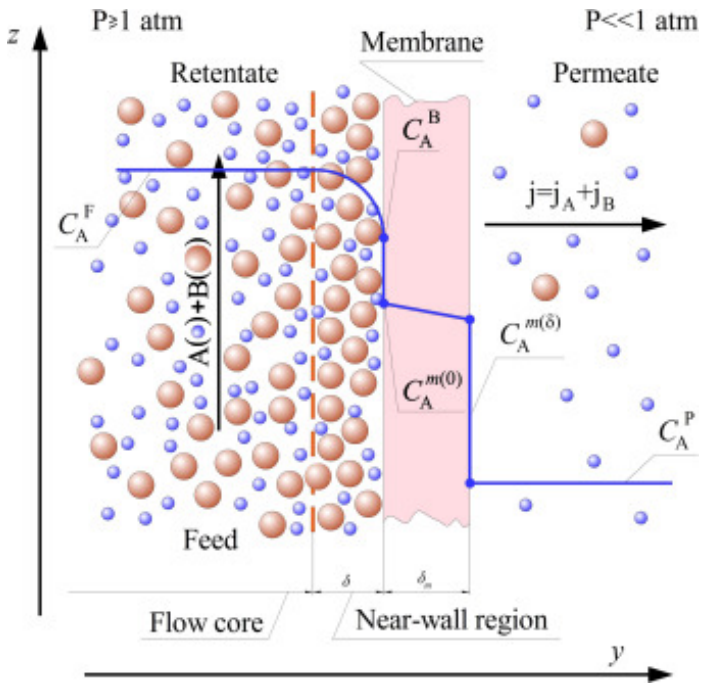

Figure 2.6: Solution diffusion model [19].

[4]This model can be divided in 3 or 5 steps depending on the reference. The steps added are the transfer from the feed stream to the boundary layer and the transfer from the layer boundary to the permeate flow. These steps are not crucial for the model and can be skipped.

Demonstration

This demonstration is inspired from: "Course about gas permeation and pervaporation" (Patricia Luis Alconero, 2017) [6].

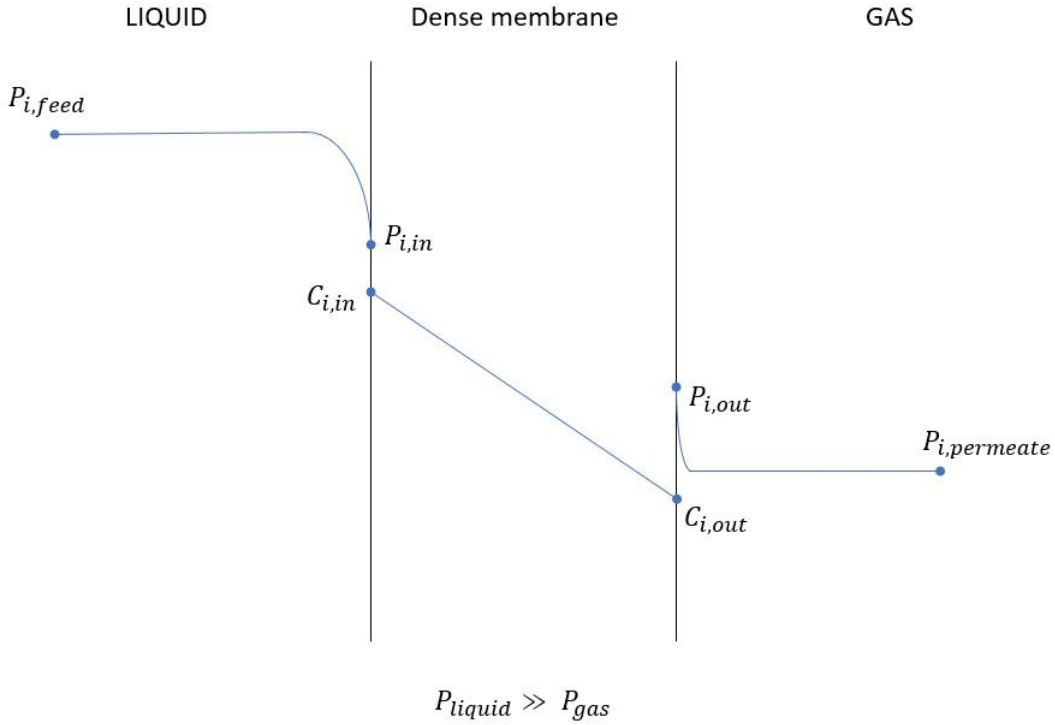

Figure 2.7: Solution diffusion model scheme.

Only sorption-diffusion-desorption is considered.

Fick's law is the foundation of this model:

$$N_i = \frac{D_i}{l_M}(c_{i,in} - c_{i,out})\left[\frac{mol_i}{s \cdot m^2}\right] \tag{2.1}$$

where D_i is the diffusion coefficient of component i, l_M is the membrane thickness, $c_{i,in}$ and $c_{i,out}$ are concentrations of the inside and outside of the membrane respectively.

The problem is that the concentration at membrane surface is not known and impossible to record. Then Henry's law is used:

$$H_{i,x} = \frac{c_{i,x}}{p_{i,x}} \tag{2.2}$$

where $H_{i,x}$ is the Henry coefficient (solubility coefficient) and x is the place (inside or outside the membrane) and $p_{i,x}$ is the partial pressure of the component i at the location x.

The Henry coefficient of each side of the membrane is assumed to be equal:

$$H_{i,in} = H_{i,out} = H_i$$

Equation 2.1 becomes:

$$N_i = \frac{D_i \cdot H_i}{l_M}(p_{i,in} - p_{i,out}) \tag{2.3}$$

Moreover, the partial pressure of the inside membrane is assumed to be at equilibrium $p_{i,in} = p_{i,feed}$ as for the outside of the membrane $p_{i,out} = p_{i,permeate}$.

Equation 2.3 becomes:

$$N_i = \frac{D_i \cdot H_i}{l_M}(p_{i,feed} - p_{i,permeate}) \tag{2.4}$$

The driving force for pervaporation is defined as the partial pressure difference:

$$Driving\ force = p_{i,feed} - p_{i,permeate}[atm]$$

where $p_{i,feed} = x_i \gamma_i P_i^0$ and $p_{i,permeate} = y_i P_p$ using Raoult's law.

Then a membrane performance coefficient can be defined from equation 2.4:

$$N_i = coefficient \cdot Driving\ force \tag{2.5}$$

The coefficient definition is:

$$Permeance = \frac{P_i}{l_M} = \frac{D_i H_i}{l_M} \tag{2.6}$$

This coefficient will be used to evaluate membrane performance in the next section.

2.2.3 Membrane performance equation

The membrane will be analysed according to three aspects [17]:

- **Membrane productivity** is determined by the permeation flux J (equation 2.7) which corresponds to the quantity of a component passing through the membrane. This property is also defined by the permeability/permeance (those concepts are explained later).

- **Membrane selectivity** is expressed by the separation factor β (equation 2.13) or selectivity α (equation 2.14) which both express the ability of the membrane to permeate only one specific compound.
- **Membrane stability** is determined by the membrane ability to sustain permeability and selectivity[5] under specific system conditions during an extended period of time.

As explained above, membrane performance evaluation is a major issue in pervaporation technology. However an important point for this evaluation is considering the driving force influence. The driving force for pervaporation is the component partial pressure difference between feed and permeate side. Therefore the analysis will be based on permeances and selectivities instead of fluxes and separation factor. Indeed permeance and selectivity are not influenced by the driving force[6] and are only membrane properties.

First of all, total flux will be computed and analysed using equation 2.7 then flux of each component will also be computed using equation 2.8 and 2.9. This way, permeance can be computed using equation 2.11. The temperature effect on permeance will be evaluated using equation 2.12. The separation factor β and selectivity α will be studied using equation 2.13 and 2.14. Finally the separation will be analysed using McCabe and Thiele Diagram (results must be taken with precaution due to the driving force effect).

First of all, the equation of permeate total flux is:

$$J = \frac{W}{At}\left[\frac{kg}{h \cdot m^2}\right] \tag{2.7}$$

where W is the weight of permeate condensed during time t and A is the effective membrane surface area.

Then flux of component i can be computed from J:

$$J_i = J \cdot y_i \frac{m_i}{m_t}\left[\frac{kg}{h \cdot m^2}\right] \tag{2.8}$$

where m_i and m_t are the molecular weight of the component i and the mixture, y_i is the permeate molar fraction.

[5] Permeability and selectivity are membrane properties while flux and separation factor are also influenced by the driving force of the experimental configuration.

[6] Therefore permeance and selectivity are not dependent on the experimental configuration.

Molar flux for each component i j_i can subsequently be computed as:

$$j_i = J_i \frac{v_i^G}{m_i} \left[\frac{m^3}{h \cdot m^2} \right] \tag{2.9}$$

where v_i^G is the molar volume of gas i, $v_i^G = 22.4 \frac{L}{mol}$ for standard temperature and pressure condition, m_i is the molecular weight of component i.

The driving force evaluation is very important in order to analyse the membrane performance. This can be evaluated through partial pressure difference between feed and permeate side as in the following equation:

$$Driving\ force = x_i \gamma_i P_i^0 - y_i P_p [atm] \tag{2.10}$$

The equation for permeance (which does not take into account the driving force) is:

$$Permeance = \frac{P_i}{l} = \frac{j_i}{Driving\ force} = \frac{j_i}{x_i \gamma_i P_i^0 - y_i P_p} \tag{2.11}$$

where $\frac{P_i}{l}$ is the permeance[7], P_i the permeability, l the membrane thickness, j_i the molar flux of i (equation 2.9), x_i the molar fraction of MeOH in the feed side, y_i the molar fraction of MeOH in the permeate side, P_p the permeate side pressure, γ_i is the activity coefficient of component i (computed from aspen) and P_i^0 vapor pressure (computed from aspen). The results of P_i^0 and γ are exposed in the ***Appendices*** Section 5.1.

The influence of temperature on permeance can be assessed by equation below:

$$\frac{P_i}{l} = \frac{P_{i,\infty}}{l} \cdot exp\left(-\frac{1000 \cdot E_a}{R \cdot T} \right) \tag{2.12}$$

where $\frac{P_{i,\infty}}{l}$ is an exponential factor, E_a the pervaporation activation energy, l the membrane thickness, R the universal gas constant and T the temperature.

The separation factor can be evaluated through:

$$\beta_{i/j} = \frac{\frac{y_i}{y_j}}{\frac{x_i}{x_j}} \tag{2.13}$$

where x_i and y_i are molar fraction of feed and permeate side respectively.

[7]Different units are possible for permeance depending on conversion : $1 \cdot \frac{m^3}{m^2 \cdot atm \cdot h} = \frac{1}{36} \cdot \frac{cm^3}{cm^2 \cdot s \cdot atm}$ or $1 GPU = 10^{-6} \frac{cm^3}{cm^2 \cdot s \cdot cmHg}$

The selectivity allows to analyse the separation performance of the membrane without taking into account the driving force. This can be calculated by:

$$Selectivity = \alpha_{i/j} = \frac{\frac{P_i}{l}}{\frac{P_j}{l}} = \frac{P_i}{P_j} \tag{2.14}$$

where $\frac{P_i}{l}$ is the permeance of component i and P_i its permeability.

Chapter 3

Results and discussion

This chapter presents the membrane performance analysis through three main aspects. First of all, the membrane productivity will be evaluated through flux and permeance. Secondly, the membrane separation ability will be analysed through separation factor and selectivity and this analysis will be confirmed by McCabe and Thiele diagram. Finally the membrane performance stability will be discussed.

3.1 Flux

On Figures 5.5 to 5.9 in ***Appendices*** Section 5.3.1, the flux evolution over time in the experiment is shown, it can be observed that there are some variations in the flux but it is nearly at steady state. The graphs also show that raising temperature increases flux, this will be detailled in the Section 3.1.2. The flux means for every concentration and temperature are summarised in Table 3.1. It is important to notice that the flux is null for MeOH 0.9 and pure MeOH.

Table 3.1: Results for the flux $[\frac{kg}{hm^2}]$ of pervaporation experiments.

	Temperature (°C)		
MeOH concentration (%mol)	40	50	60
0	0.61885	0.76345	0.8605
10	0.10995	0.11	0.21585
30	0.04533	0.1823	0.3918
50	0.29695	0.3336	0.359
70	0.1693	0.25315	0.2621
90	0	0	0
100	0	0	0

3.1.1 Flux over concentration analysis

With the results shown on Table 3.1 for every experiments, an analysis of the feed concentration effect on flux can be done. The results are shown on figure 3.1.

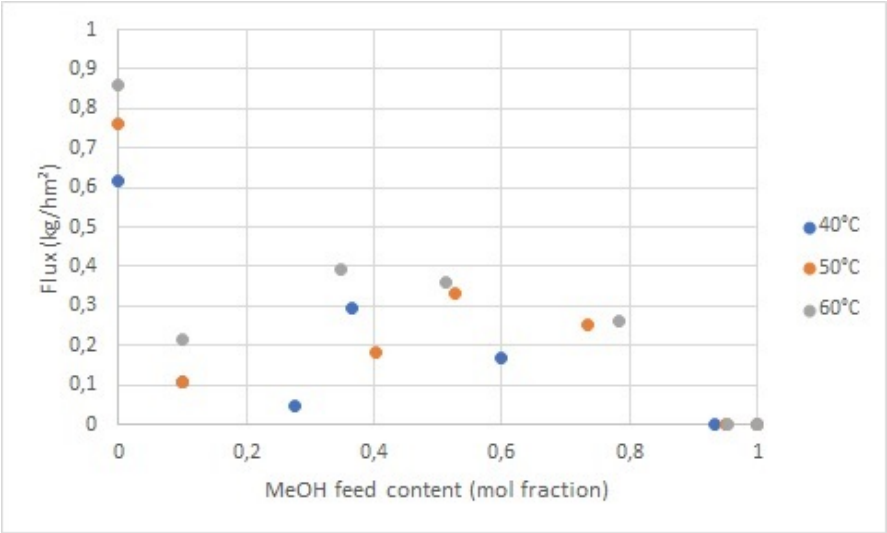

Figure 3.1: Flux evolution over concentration for different temperatures.

From Figure 3.1, it is obvious that DMC permeates more easily than MeOH. In addition, overall trend shows that flux is inversely related to MeOH concentration.

Data at 10%mol and 30%mol MeoH are not meaningful. It should be due to the fact that membrane performance results are not stable and steady as exposed in Section 3.7.

The permeation and the separation depend on the membrane selective layer. However selective layer material is unknown as it is a commercial membrane. Therefore analysis on the membrane can not be done to know why DMC passes through.

3.1.2 Flux over temperature analysis

With the results shown on Table 3.1 for the different experiments, an analysis of the temperature effect on flux can be done. The summary is shown on figure 3.2 and the results for each concentration are shown on Figures 5.10 to 5.13 in ***Appendices*** Section 5.3.2.

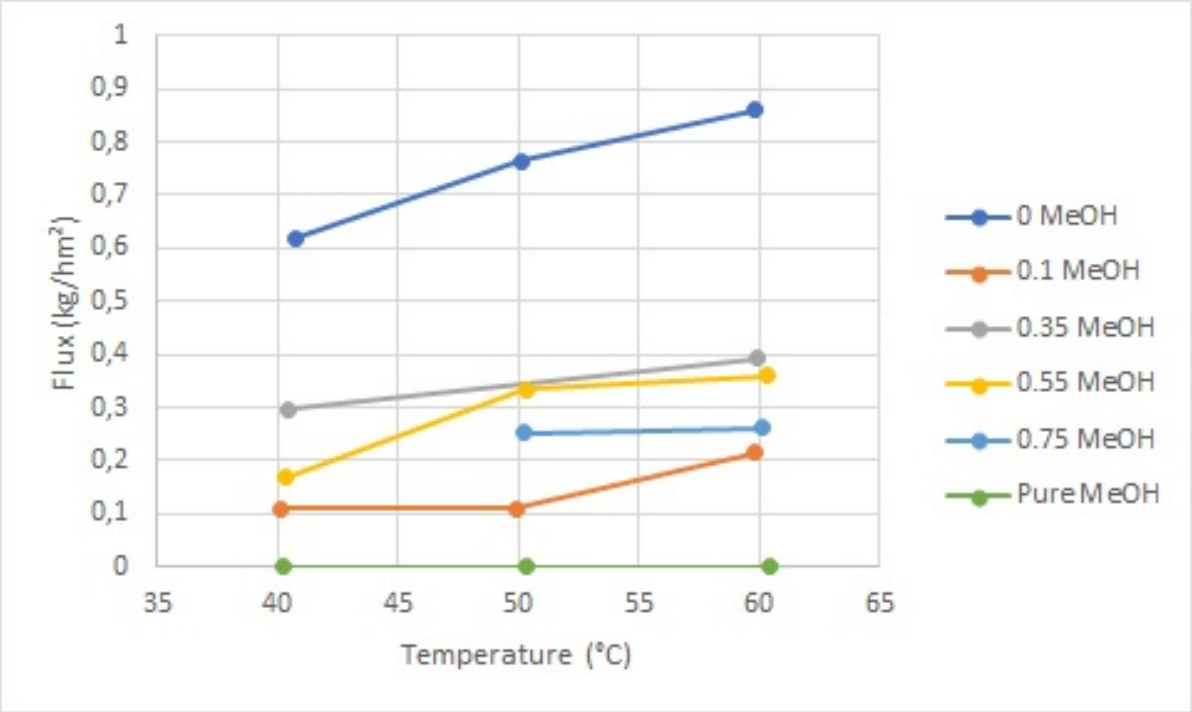

Figure 3.2: Flux evolution over temperature for different feed solutions (MeOH mole fraction).

It can be observed that this flux evolution raises with temperature. Sections 3.1.3 and 3.1.4 show that the flux of each component increases with the temperature. Therefore the total flux relation with temperature is coherent as the flux is the sum of each component flux.

3.1.3 Flux of MeOH

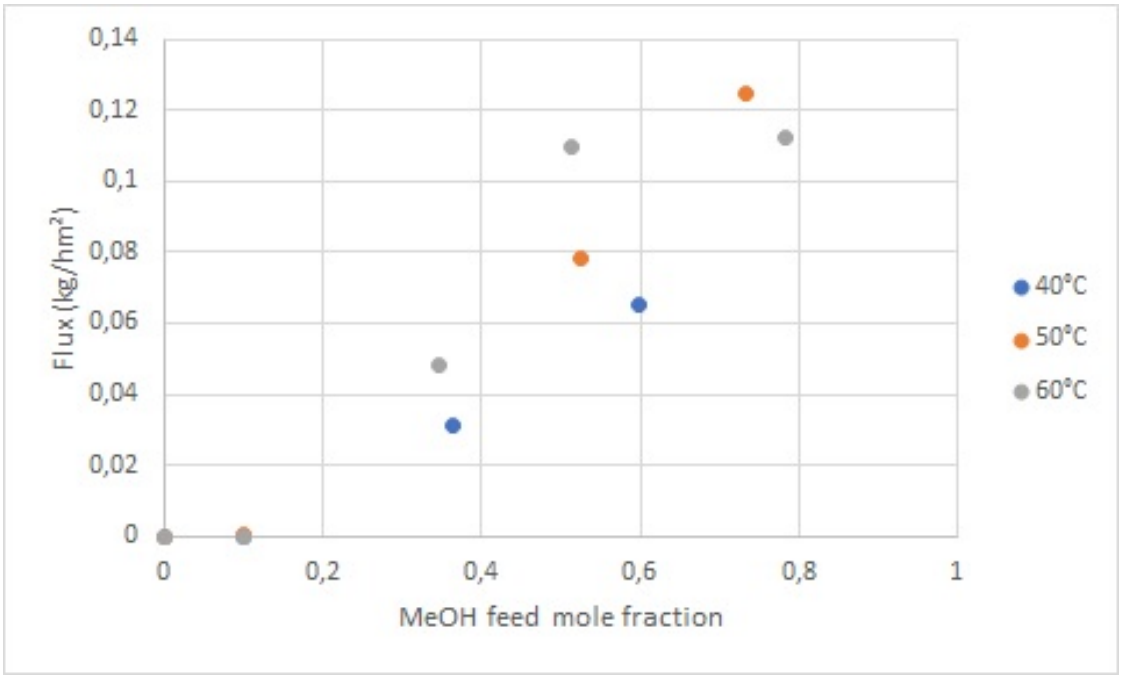

Figure 3.3: MeOH flux evolution depending on MeOH feed content (MeOH mole fraction) and temperature.

Figure 3.3 exhibits the methanol flux depending on temperature and concentration. As that can be anticipated, the methanol flux increases with the methanol mole fraction. Furthermore it can be noticed that increasing temperature also raises the flux. Thgourgh the figures 3.4 to 3.6, an explanation of the link between flux and temperature will be given.

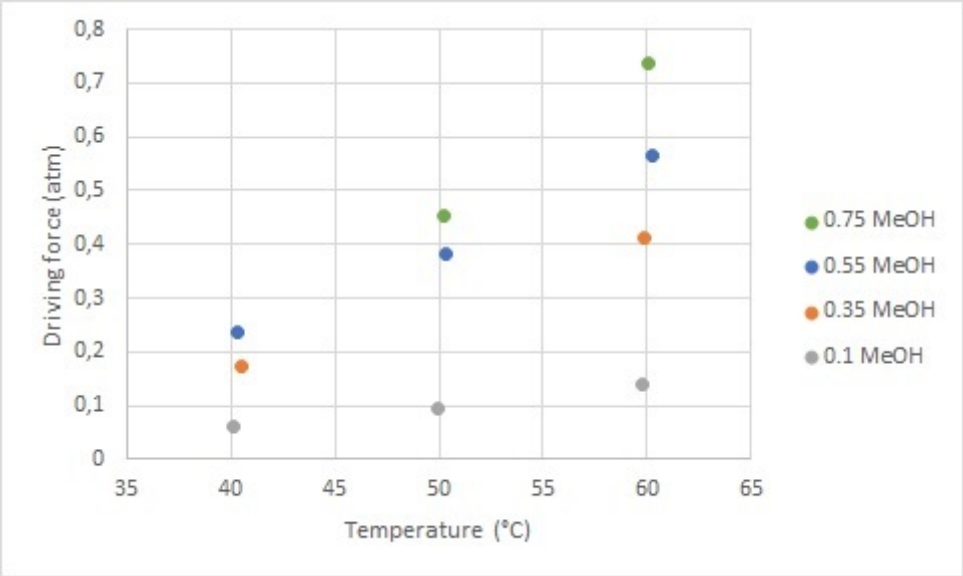

Figure 3.4: Methanol driving force evolution according to temperature and MeOH feed content (MeOH mole fraction).

In order to understand easily the following point, here is a reminder of the flux equation (using solution-diffusion model in Section 2.2.2):

$$J_i = \frac{P_i}{l}(x_i \gamma_i P_i^0 - y_i P_p) \tag{3.1}$$

Two observations can be done about Figure 3.4. On one side, methanol driving force increases with the methanol concentration. Indeed this increase is justified by equation 2.10: methanol driving force increases with x_i. On the other hand, the driving force raises with temperature. The vapour pressure P^0_{MeOH} increases more than activity coefficient decreases with temperature as it is shown on Figure 3.5.

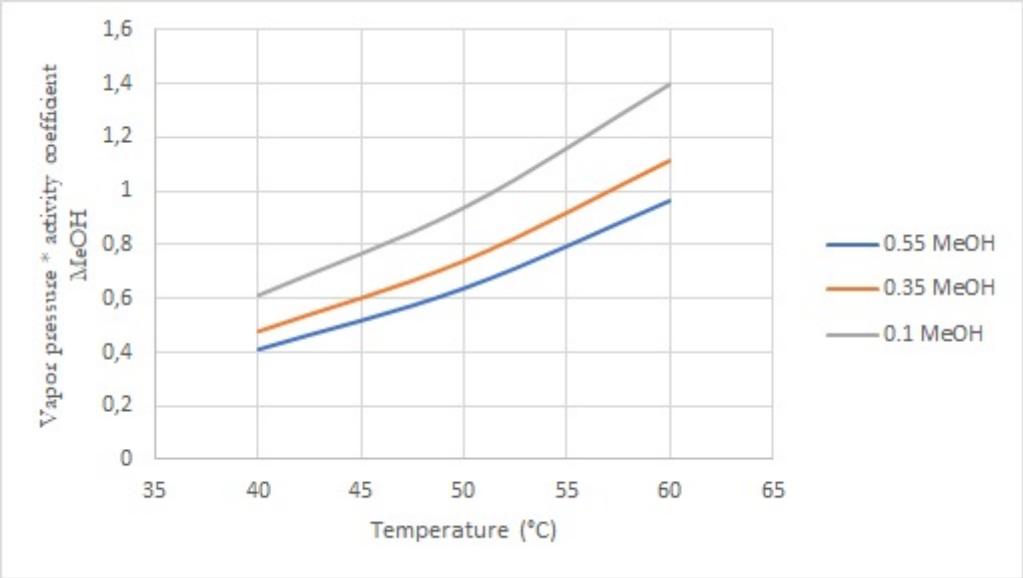

Figure 3.5: $\gamma_{MeOH} \times P^0_{MeOH}$ depending on temperature for different feed solutions (MeOH mole fraction).

The temperature evolution can be analysed using this equation: $Flux = driving\ force \times Permeance$. The impact due to the temperature increase is lower for permeance than for driving force. Indeed, as shown on Figures 5.14, the permeance declines by around 20% for each increase of 10 $°C$. On the other hand, as shown on figure 3.4, the driving force increases by around 50% for each increase of 10 $°C$. That's why the flux will increase with by around 30% temperature and the cause of flux raising is the driving force.

The evolution of driving force with temperatures can be understood as follow. The feed concentration x_i is constant. temperature does not have a significant influence on the permeate concentration y_i as shown on Figure 3.15. Therefore the temperature influence on flux is mainly due to the activity coefficient γ_i and vapour pressure P^0_i.

$\gamma_i \times P^0_i$ is shown on Figure 3.5. This figure can explain the flux increase with temperature. Indeed $\gamma_i \times P^0_i$ raises with temperature then driving force and flux increase with temperature.

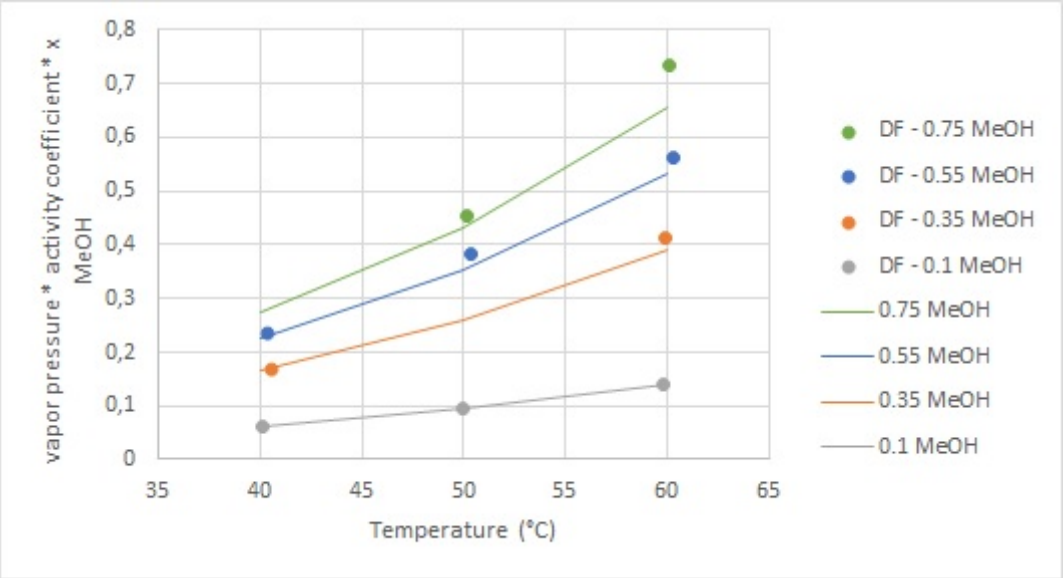

Figure 3.6: Theoretical values: $\gamma_{MeOH} \cdot P^0_{MeOH} \cdot x_{MeOH}$ depending on temperature and MeOH feed content (MeOH mole fraction) (lines). Experimental values: methanol driving force depending on temperature and on feed content (points).

In conclusion the temperature influences significantly the methanol flux due to the driving force especially $x_i \gamma_i P_i^0$ part.

Driving force is not only membrane dependant. The parameters influenced by the driving force as flux are consequently not exclusively dependant on the membrane. In order to avoid driving effect, permeance is used as it equals $\frac{Flux}{Diving\ force}$. Hence permeance which is an intrinsic membrane performance parameter will be computed in a next section.

3.1.4 Flux of DMC

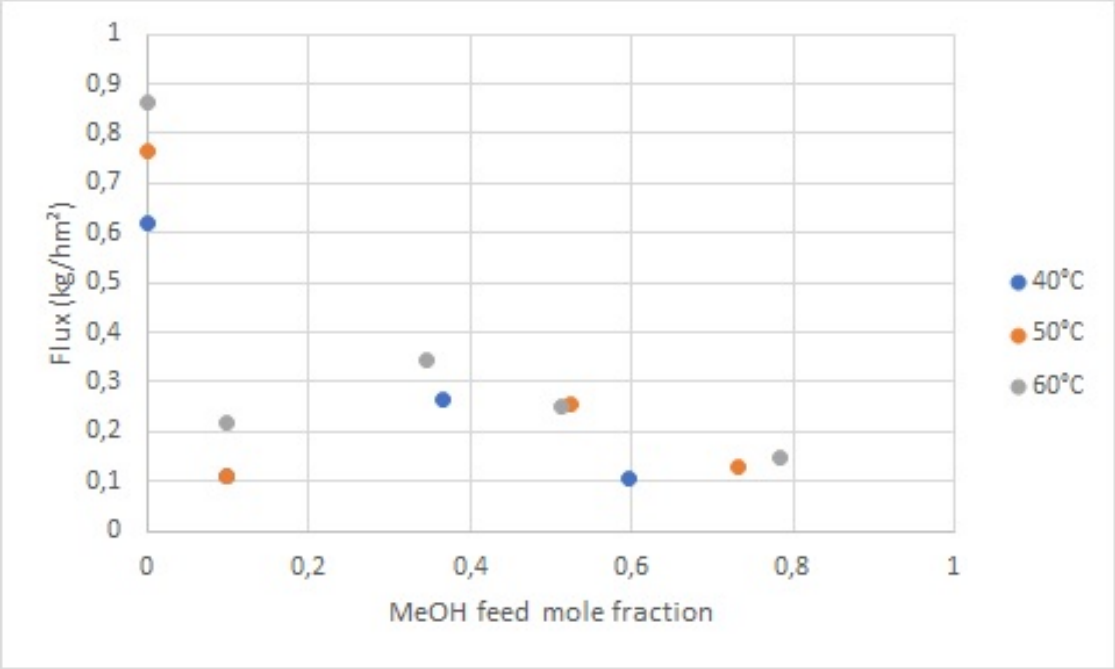

Figure 3.7: DMC flux evolution depending on MeOH feed content (MeOH mole fraction) and temperature.

The same analysis as for the methanol flux (Section 3.1.3) can be done. The increase of flux with temperature can also be ascribed to the evolution of driving force with temperature.

The opposite trend of methanol is displayed on Figure 3.7. Indeed increasing methanol content reduces the DMC flux. This can be explained by flux equation 3.1: x_i decreases then the DMC driving force decreases as DMC flux.

The results for 10%mol MeOH are not significant. It could be allocated to the lack of membrane performance stability as exposed in Section 3.7.

3.2 Permeance

The permeance indicates which component permeates through the membrane without taking into account the driving force.

3.2.1 Methanol permeance

Figure 3.8 displays the increasing of methanol permeance with the feed methanol content.

To conclude the membrane permeates methanol from a threshold and the permeation increases with methanol concentration. However pure methanol does not permeate. Two factors can explain the methanol permeance trend:

- The membrane stability can be an explanation as every results are uncertain.
- This phenomena can be understood by the coupling effect. Methanol permeation depends on DMC permeation. Indeed the affinity of MeOH is apparently linked with the DMC presence.

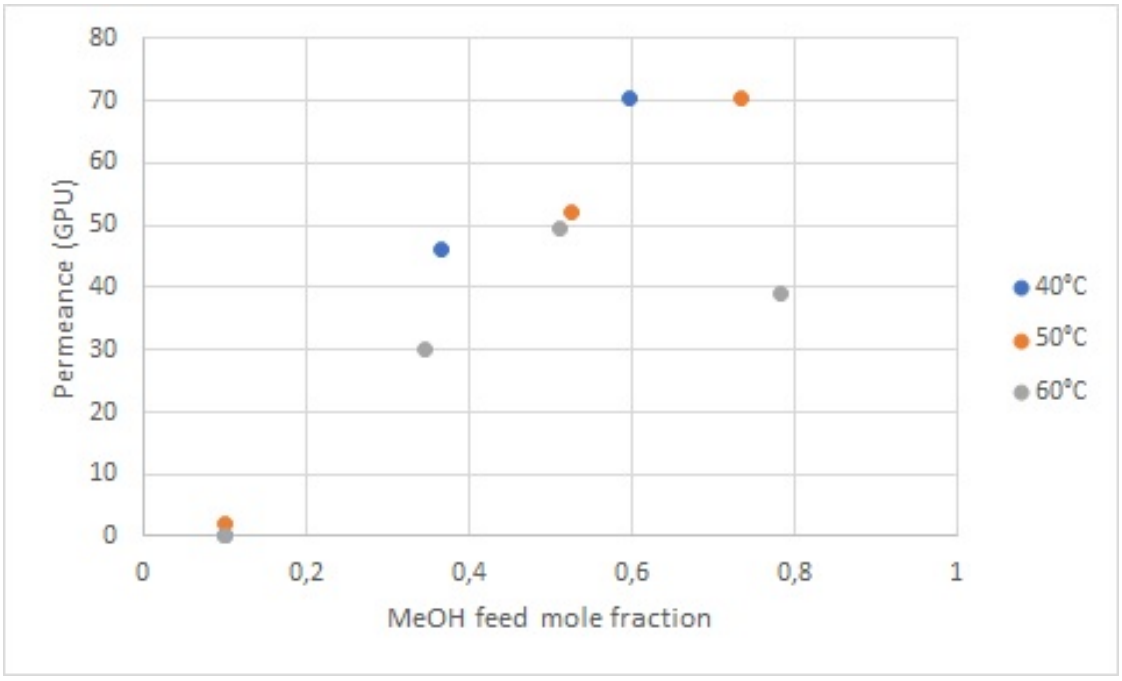

Figure 3.8: MeOH permeance evolution depending on temperature and MeOH feed content (MeOH mole fraction).

3.2.2 DMC permeance

First of all, it can be observed on Figure 3.8 and 3.9 that DMC permeance is bigger compared to MeOH permeance. As said before, the selective layer is unknown so an explication to understand why DMC permeates more than MeOH can not be given.

Thereafter permeance decreases logically with the feed MeOH content. Indeed, DMC permeation decreases with the DMC feed mole fraction decreases. Once more, the results for 30%mol MeOH can be discarded due to the lack of performance stability as explained in Section 3.7.

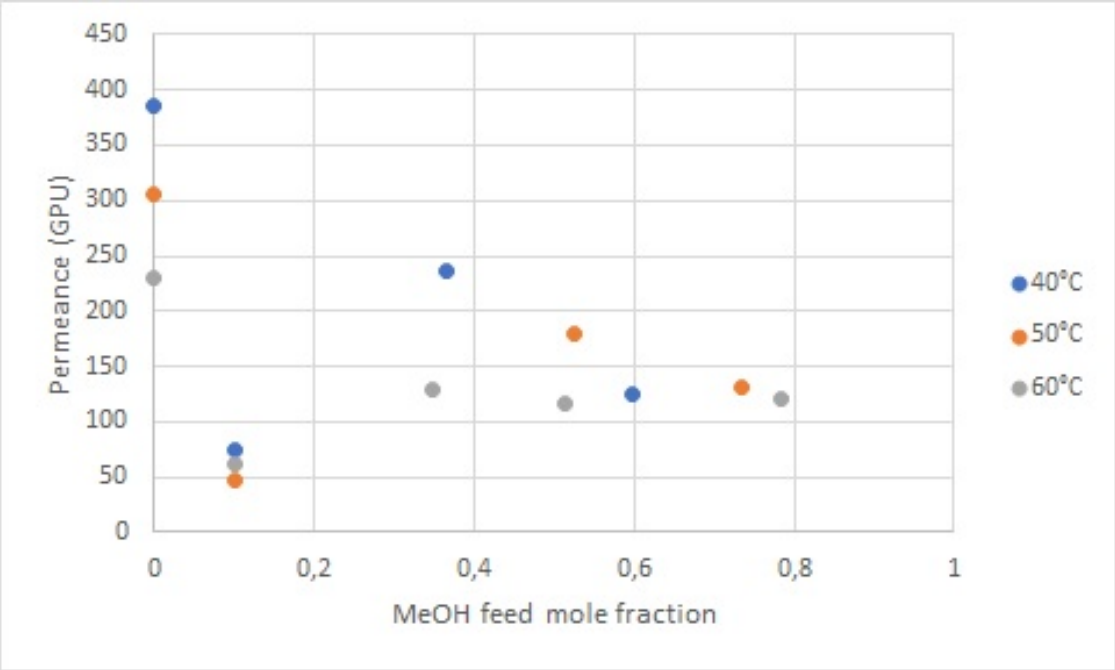

Figure 3.9: DMC permeance evolution depending on temperature and MeOH mole fraction (MeOH mole fraction).

3.2.3 Evolution with temperature

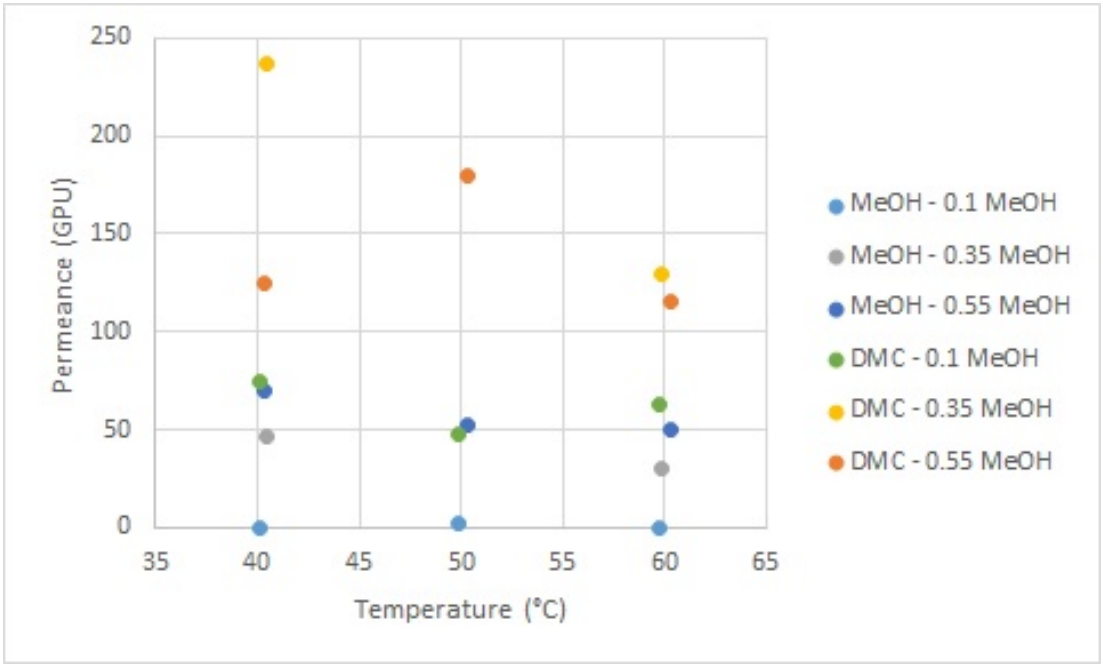

Figure 3.10: Permeance evolution of DMC and MeOH depending on temperature and MeOH feed content (MeOH mole fraction).

Global trend shows that permeance decreases with temperature for MeOH and DMC. The Section 3.2.4 will reveal the origin of this reduction.

3.2.4 Activation energy E_a

The permeance can be analysed by the pervaporation activation energy E_a. Equation 2.12 can be modified in order to compute activation energy E_a:

$$\ln \frac{P_i}{l} = \ln \frac{P_{i,\infty}}{l} - \frac{1000 \cdot E_a}{RT}$$

A plot of $\ln \frac{P_i}{l}$ over $\frac{1000}{RT}$ is needed to have the slope which is equal to $-E_a$ and the y-intercept which is equal to $\ln \frac{P_{i,\infty}}{l}$.

The figures below will help computing this two factors.

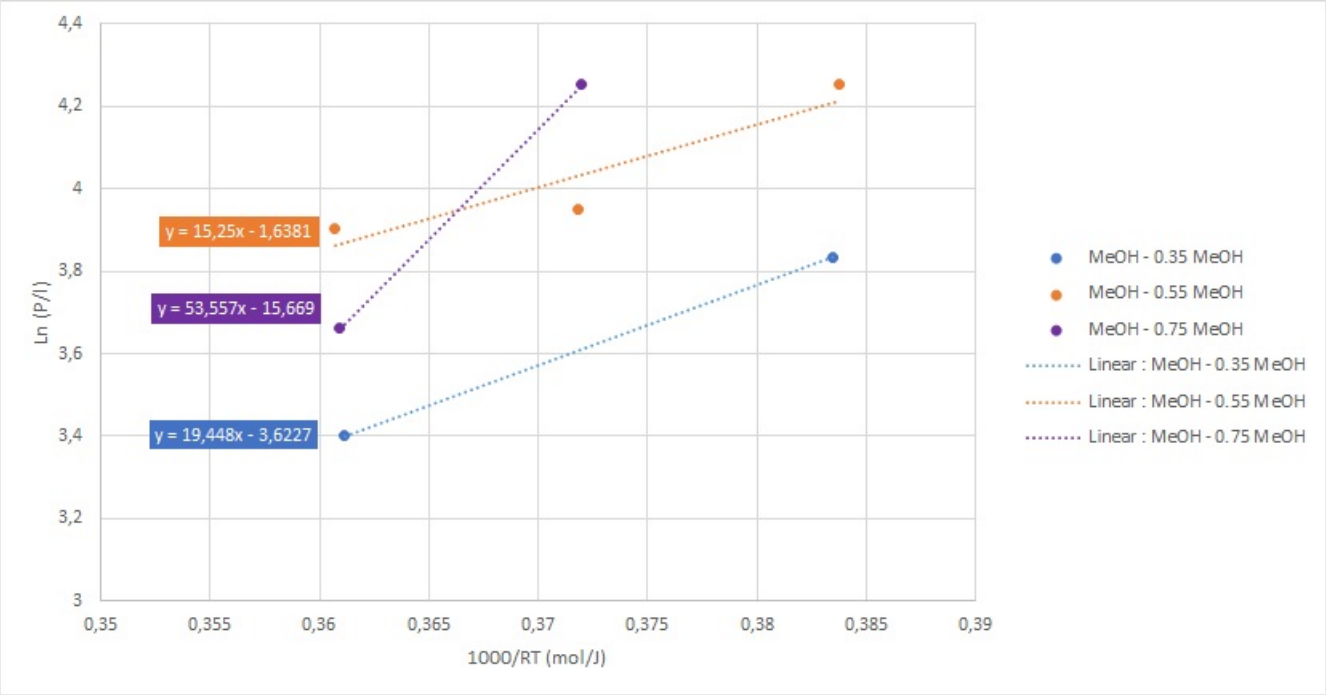

Figure 3.11: $\ln \frac{P_{MeOH}}{l}$ **over** $\frac{1000}{RT}$ **in order to compute** $E_{a,MeOH}$ **for different feed solutions (MeOH mole fraction).**

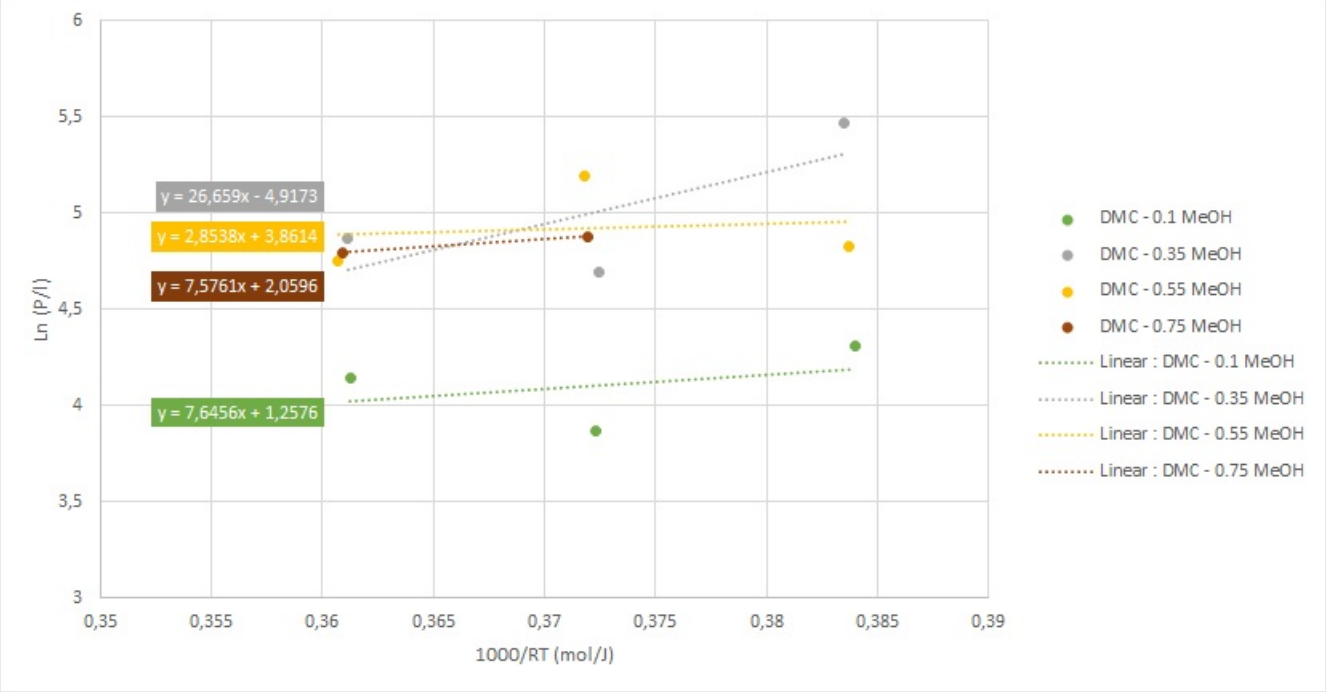

Figure 3.12: $\ln \frac{P_{DMC}}{l}$ **over** $\frac{1000}{RT}$ **in order to compute** $E_{a,DMC}$ **for different feed solutions (MeOH mole fraction).**

The data given on Table 3.2 are computed from Figures 3.11 and 3.12.

Table 3.2: Activation energy E_a calculation.

Feed content $[\%molMeOH]$	DMC E_a $\left[\frac{J}{mol}\right]$	DMC $\frac{P_{i,\infty}}{l}$ [GPU]	MeOH E_a $\left[\frac{J}{mol}\right]$	MeOH $\frac{P_{i,\infty}}{l}$ [GPU]
10	- 7.6456	3.5170		
35	- 26.659	0.0073	-19.448	0.0267
55	-2.8538	47.532	-15.25	0.1943
75	-7.5761	7.8428	-53.557	$\simeq 0$
AVERAGE	**-11.1836**	**14.725**	**-29.4183**	**0.0737**
Modified average	-6.025	19.351	-17.349	0.1105

First of all, all the pervaporation activation energy is negative. In ***Appendices*** Section 5.3.3, the figure 5.14 presents permeance evolution using the modified mean activation energy. The modified average has been taken in order to skip meaningless data. The trend of the curve generally matches with the data trend. The curve is a bit higher compared with the data. Indeed the mean of the pre-exponential factor has a significant influence on the location of the curve.

The E_a negative values can be discussed from the equation below:

$$E_a = E_{D,i} + \Delta H_i \tag{3.2}$$

where $E_{D,i}$ is the activation energy for diffusion (generally positive) and ΔH_i is the sorption enthalpy (usually negative for exothermic sorption process) [26].

The activation energy is negative. Consequently sorption enthalpy absolute value is higher than $E_{D,i}$ absolute value.

Using equation 2.12, it is obvious that negative E_a indicates a permeance depletion with temperature.

This has demonstrated that the permeance decreases with temperature (as exposed in Section 3.2.3).

On the other hand, Table 3.2 suggests that E_a is bigger (absolute value) for MeOh than DMC. Thus methanol permeation is more impacted by the temperature variation.

3.3 Permeability

The permeability can't be calculated accurately. Indeed, the membrane thickness is not given and hard to obtain. The selective layer thickness can be assumed to be the membrane thickness as the separation occurs in this layer. The selective layer thickness is around 200 nm [29].

3.4 Separation factor $\beta_{\frac{DMC}{MeOH}}$

This factor expresses the membrane ability to permeate only one of the two components.

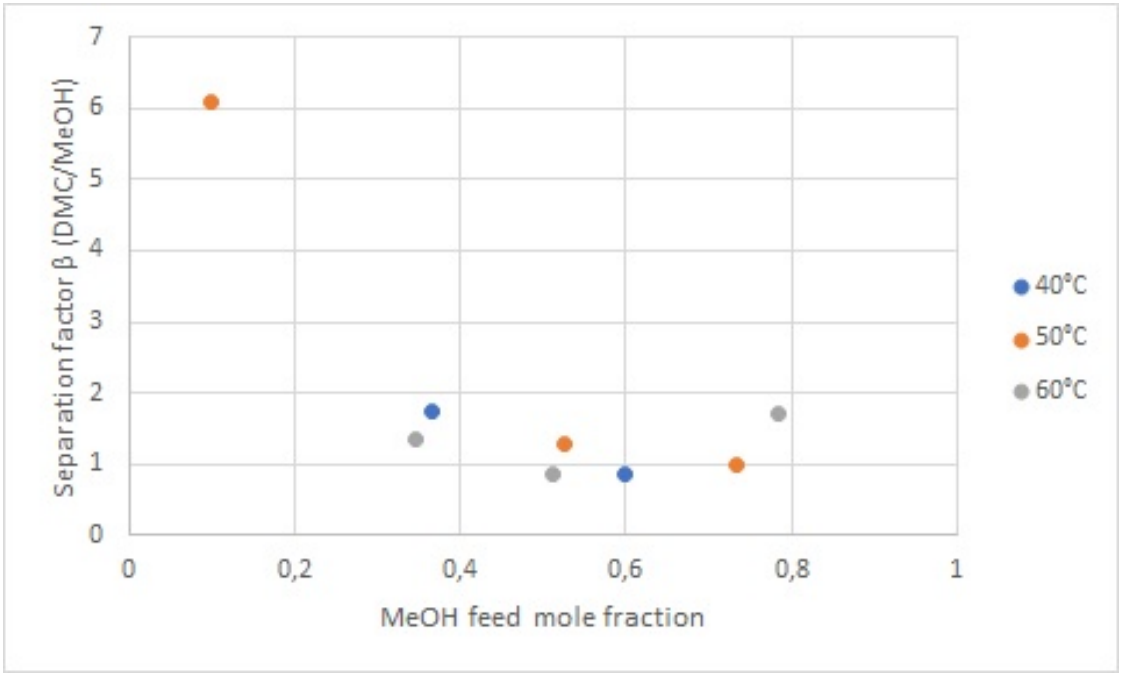

Figure 3.13: Separation factor $\beta_{\frac{DMC}{MeOH}}$ depending on temperature and MeOH feed content (MeOH mole fraction).

The value approximately equals to 1 generally[1]. This results is not successful. Indeed it means that separation is not well done. No general trend can be determined for the temperature evolution.

[1]The value of 10% MeOH feed content is not taken into account as the membrane performance stability is very low.

3.5 Selectivity $\alpha_{\frac{DMC}{MeOH}}$

The value generally[2] lay between 1 and 5 . The selectivity $\alpha_{\frac{DMC}{MeOH}} > 1$ then DMC permeates more then MeOH. However $\alpha_{\frac{DMC}{MeOH}}$ is not very high so the separation is not optimal. No general trend can be determined for the temperature evolution.

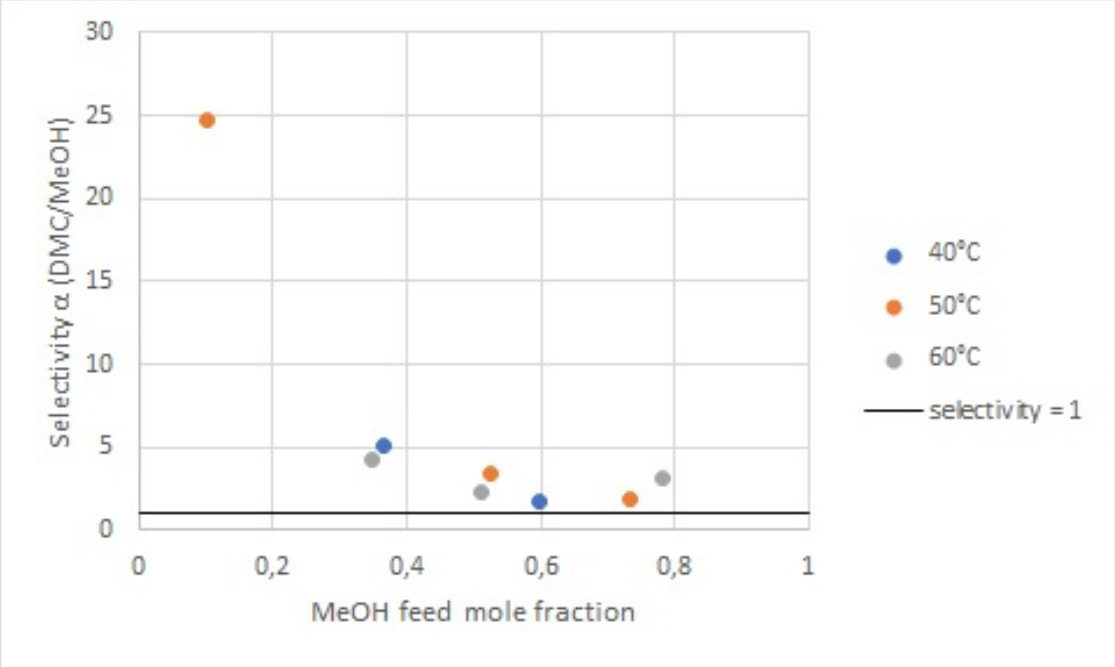

Figure 3.14: Selectivity $\alpha_{\frac{DMC}{MeOH}}$ depending on temperature and MeOH feed content(MeOH mole fraction).

3.6 Mac Cabe and Thiele diagram

This section must be analysed carefully. The next paragraphs compare separation through pervaporation and distillation.

On one hand, the distillation is evaluated by the VLE curve[3]. This curve is obtained by Aspen (at 1 bar), it is detailed in ***Appendices*** Section 5.1.3. The VLE curve shows the vapour and liquid equilibrium which takes place in the distillation column. An example of distillation column using this curve is shown in ***Appendices*** Section 5.2. Basically, liquid composition can be understood as feed and vapour composition as the output.

[2]The value of 10% MeOH feed content is not taken into account as the membrane performance stability is very low.

[3]This VLE curve does not look like the curve in Section 1.3 because here it is in mass fraction.

On the other hand, the pervaporation is analysed by the output composition depending on feed content.

3.6.1 Comparison with distillation

The VLE curve corresponds to the distillation performance. As shown in Section 1.3, distillation is not an optimal solution. The separation through pervaporation using HybSi membrane is also not efficient. Indeed the results show that separation does not occur. The temperature does not influence significantly the separation as shown on Figure 3.15.

For high concentrated DMC mixture, the permeate is only made of DMC. It is not very pertinant because the permeate flux is low then only small quantity of pure DMC can be obtained and the rest of the retentate will remain a binary mixture.

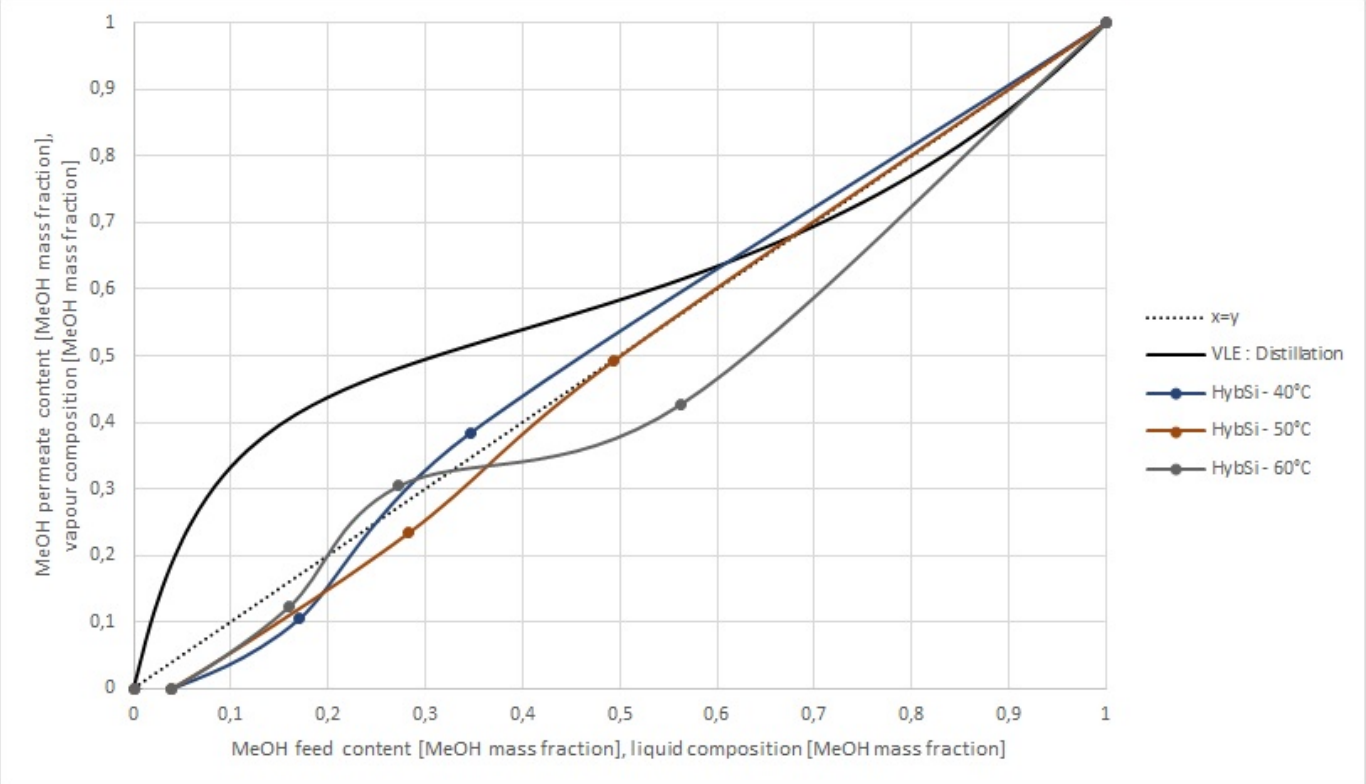

Figure 3.15: McCabe and Thiele diagram gives permeate mole fraction depending on feed mass fraction of MeOH (MeOH mass fraction).

It can be concluded that the pervaporation using HybSi membrane is not a good separation technique.

3.6.2 Comparison with other membranes

Figure 3.16 indicates the differences between several membranes for DMC-MeOH separation.

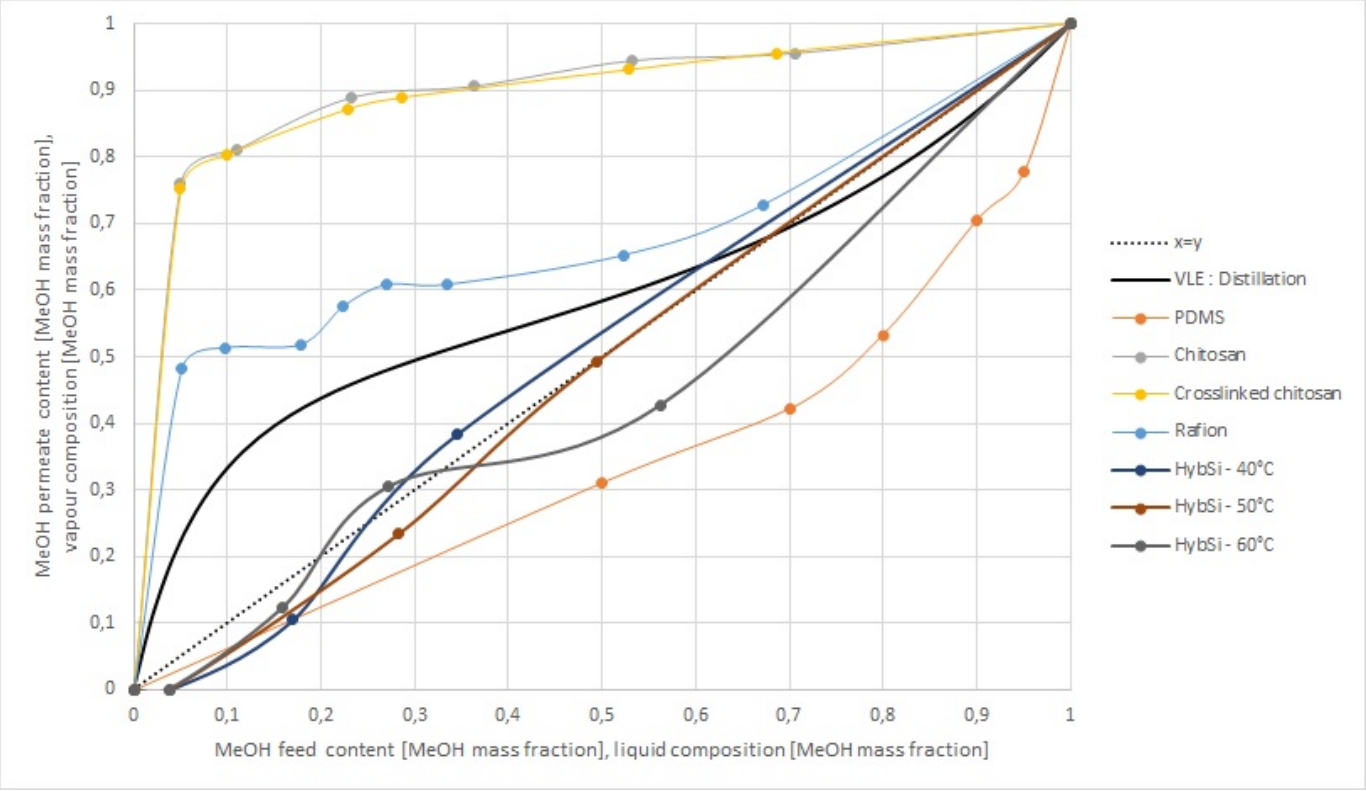

Figure 3.16: McCabe and Thiele diagram gives permeate mole fraction depending on feed mass fraction of MeOH (MeOH mass fraction) for several membranes. Orange line is a PDMS membrane [36], grey line is chitosan membrane [39], yellow line is crosslinked chitosan membrane [40] and Nafion® is in blue [20].

Figure 3.16 highlights two relevant facts.

First of all, the HybSi membrane is not performant compared to other ones.

Secondly, Chitosan membranes (crosslinked or not) are the most interesting subject to explore, the separation is the best through this membrane. The major application can be MeOH removal from DMC. Indeed, for low concentration of methanol in the feed, the permeate is mainly made of methanol which can lead to DMC purification at the feed/permeate side.

3.7 Membrane performance stability

Some experiments have been done a second time (MeOH 0%mol and MeOH 30%mol) but flux was very low/null.

Then the membrane has been cleaned with ethanol and new experiments with MeOH 0%mol and MeOH 50%mol have been done, the flux was still null.

Finally the membrane has been immersed in DMC during 72 hours. Pervaporation experiments (MeOH 0%mol and MeOH 30%mol) have been done again however the flux was still null. The reproducibility results are shown on Table 3.3

Membrane	Composition $[\%mol]$MeOH	Temperature $[°C]$	Flux $[\frac{kg}{h \cdot m^2}]$
Membrane used	30	40	0.0736
	30	50	0.077
	30	60	0.1112
Membrane cleaned with ethanol	0	40-60	0
	0	40-60	0
	50	40-60	0
Membrane immersed in DMC	0	40-60	0
	30	40-60	0

Table 3.3: Reproducibility of the experiments.

The membrane performances can not be repeated. These results exhibit a relevant problem of the membrane which will be discussed in Section 3.8.

Only the results of experiments from Table 3.1 have been taken into account for the previous computations.

3.8 General results discussion

As explained previously, the membrane performance results indicate low membrane efficiency. This section will compare this study results to others found in literature. Table 3.4 picks up the results obtained during laboratory experiments.

3.8.1 Results analysis

Conditions		Results	
Feed composition $[\%wt\ MeOH]$	Temperature [°C]	Flux $\left[\frac{kg}{h \cdot m^2}\right]$	Separation factor $\beta_{\frac{DMC}{MeOH}}$
34.6	40.3	0.1693	0.84
28.3	50.325	0.3336	1.2886
27.2	60.3	0.359	0.8526
49.4	50.2	0.25315	1.004
56.2	60.1	0.2621	1.722

Table 3.4: Summary of membrane performance results.

Comparison with other HybSi membrane applications

HybSi membrane is mainly used for dehydration as mentioned on Table 1.3 in Section 1.6 [19] [29] [27]. This table shows the dehydration performance results. The separation factors obtained in these studies are very high (120-10000). The flux lies between 0 to 10 $\left[\frac{kg}{h \cdot m^2}\right]$. To sum up, this membrane can be used for industrial dehydration as this application results are pertinent.

HybSi membrane has also been used for ammonia removal from water [41]. However the results of flux and separation factor are less performing compared to dehydration one.

Comparison with other membranes used for MeOH-DMC separation

Three membrane types have been quoted in the Section 1.4.2: PDMS [42] [36], Chitosan [10] [40] [39] [9] and Nafion [20]. Their performance results are illustrated on Table 1.2. The separation factor of these three membranes is always higher than then separation factor for HybSi membrane. The flux for low temperature (35-50 °C) is generally less then 1 $\left[\frac{kg}{h \cdot m^2}\right]$ for every membranes.

Intermediate conclusion

In conclusion, HybSi membrane is apparently high-performance for dehydration. Studies have shown that MeOH-DMC separation by pervaporation is possible.

To conclude about this present document, HybSi membrane attests low flux through the membrane which seems normal by comparison with other articles results. The separation is not very efficient compared to other studies as mentioned in the last two sections. To sum up, the HybSi membrane does not allow separating efficiently DMC and MeOH.

3.8.2 Membrane stability

As reported in Section 3.7, the membrane performances are not stable. Due to this instability the results computed above can not be used as a reference because experiments results are not reproducible.

Different possible phenomena can explain the flux decrease.

First of all, there is no link to the membrane itself, a pervaporation test has been done during three years without any damages to the membrane. This experiment recorded the water and n-butanol separation at 150°C. Attention must be paid, this test has been done by gas permeation but it only shows the membrane structure stability [35].

Silica membranes have already been used with MeOH without any problems. The experimental conditions are: 30-80 °C, 5-22% water in MeOH [11]. Then the MeOH interaction with the membrane can not be a reason of the flux instability.

The explanation could be that the membrane undergoes a modification or is not suitable for pervaporation. Three possibilities are quoted below:

1. **Contamination**:

   The membrane supplier gave this explanation. However after membrane cleaning and despite the high purity of feed mixture the flux is still null. Consequently this explanation has not been proven.

2. **Membrane application**:

   The membrane supplier announced that the membrane can be used both for pervaporation and vapour permeation. The results obtained in this document show that pervaporation for DMC-MeOH separation using HybSi membrane is not successful. This membrane could be not appropriate for pervaporation but only for gas permeation. Gas permeation is a totally different process. Indeed the feed is at vapour phase consequently there is no phase transformation through the membrane. While this could be a reason, some articles prove that pervaporation wokrs using HybSi membrane with other components than DMC and MeOH [19], [29], [27] and [41].

3. **DMC-membrane interaction**:

   The supplier does not give information about the selective layer composition. It could be possible that DMC reacts with this material. The membrane may have changed which results in preventing components to pass through.

As a conclusion more tests with the membrane are required the reasons why the membrane is not stable. For example, a test with water to verify it it permeates through the membrane (water permeation through HybSi membrane is proven in several articles). In case of permeate flux, it is then proved that this membrane is not suitable for DMC-MeOH separation through pervaporation.

A test at higher temperature[4] can be planned to record permeation. In case of flux, it is then proved that vapour permeation should be preferred for this membrane.

The last experiment which could be done with this membrane is a SEM[5] to verify if the membrane undergoes modifications. This way, contamination or results of any reaction could be detected. As the membrane being very expensive, this test which requires to break it has not been done.

[4]It could not be recorded as gas permeation. Indeed, the set up does not allow vapour permeation. The installation can not ensure that only vapour is inside and liquid is not authorised for vapour permeation.

[5]Scanning electron microscope.

Chapter 4

Conclusion

The goal of this study is to analyse the DMC-MeOH separation efficiency by pervaporation using HybSi membrane.

The total flux obtained lies between 0 and 0.86 $\left[\frac{kg}{hm^2}\right]$. The flux of the membrane is low but it is not its major limitation. Its main drawback is the low separation efficiency expressed by separation factor which is between 0.85 and 1.74. It demonstrates that the membrane does not separate DMC and methanol. This lack of separation has also been illustrated through McCabe and Thiele diagram. The permeate concentration is nearly the same as the feed one.

On one hand, the membrane performance results are influenced by temperature. First the flux is increased by the temperature. This is mainly caused by the driving force evolution. Secondly temperature evolution reduces permeance. This is explained by the negative pervaporation activation energy of the membrane.

On the other hand, molar concentration evolution has also an impact on the performance. It has been shown that increasing one component mole fraction enhances its permeance and flux. This analysis reveals a coupling effect between methanol and DMC. Indeed, the methanol affinity with the membrane increases with the DMC mole fraction evolution.

Two major drawbacks about this membrane application has been reported in this document. First of all the separation is not successful. Secondly, as the data are not reproducible, it can be concluded that the membrane is not chemically stable for these components and the results obtained previously can not be generalised. To sum up, this membrane is not suitable for the separation of DMC and MeOH by pervaporation.

To go further in the understanding why the membrane is not stable, several assumptions have been made. The membrane could be inappropriate to pervaporation. The membrane structure may have been modified through contamination or a reaction with the mixture. Several other experiments as water pervaporation, high temperature test or structure analysis by SEM could be performed to verify one of the assumptions.

Bibliography

[1] European biodiesel board. http://www.ebb-eu.org/stats.php.

[2] Glycerolcarbonaat. https://nl.wikipedia.org/wiki/Glycerolcarbonaat, 2017.

[3] http://www.hybsi.com/, 2018.

[4] R. R. Akberov, A. R. Fazlyev, A. V. Klinov, A. V. Malygin, M. I. Farakhov, V. A. Maryakhina, and S. M. Kirichenko. Dehydration of diethylene glycol by pervaporation using hybsi ceramic membranes. 2013.

[5] Patricia Luis Alconero. Course about advanced distillation, 2017.

[6] Patricia Luis Alconero. Course about gas permeation and pervaporation, 2017.

[7] PERVATECH BV. Datasheet: 1-channel hybrid silica membranes. http://pervaporation-membranes.com/wp-content/uploads/2014/10/Datasheet-1-Channel-Hybrid-Silica-membranes-Version-27-05-2014.pdf.

[8] PERVATECH BV. Membranes. http://pervaporation-membranes.com/products/membranes/, 2014.

[9] Jian Hua Chen, Qing Lin Liu, Jun Fang, Ai Mei Zhu, and Qiu Gen Zhang. Composite hybrid membrane of chitosan–silica in pervaporation separation of meoh/dmc mixtures. 2007.

[10] Jian Hua Chen, Qing Lin Liu, Ai Mei Zhu, Qiu Gen Zhang, and Jun Fang. Pervaporation separation of meoh/dmc mixtures using sta/cs hybrid membranes. 2008.

[11] Johan E.ten Elshof, Cristina Rubio Abadal, Jelena Sekulić, Sankhanilay Roy Chowdhury, and Dave H.A.Blank. Transport mechanisms of water and organic solvents through microporous silica in the pervaporation of binary liquids. 2003.

[12] Institute for Sustainable Process Technology. Ispt/nl guts techno projects break down barriers. http://www.ispt.eu/media/Pervatech_projects-breakdown-barriers.pdf.

[13] Goulven G.Paradis, Donough P.Shanahan, Robert Kreiter, Henk M.van Veen, Hessel L.Castricum, Arian Nijmeijer, and Jaap F.Vente. From hydrophilic to hydrophobic hybsi® membranes: A change of affinity and applicability. 2013.

[14] Castricum H.L., Paradis G.G., Mittelmeijer-Hazeleger C.M., Kreiter R., Vente J.F., and Ten Elshof J.E. Tailoring the separation behavior of hybrid organisilica membranes by adjusting the structure of the organic briding group. *Advanced functional materials journal*, 2011.

[15] Chi-Chih Hu and Shueh-Hen Cheng. Development of alternative methanol/dimethyl carbonate separation systems by extractive distillation, a holistic approach. 2017.

[16] Agirre I., Belén Güemez M., Motelica A., M. van Veen H., F. Vente J., and L. Arias P. A techno-economic comparison of various process options for the production of 1,1-diethoxy butane. 2011.

[17] J. V. Rojas R. M. Filho J. H. Bermudez Jaimes, M. E. T. Alvarez. Pervaporation: Promissory method for the bioethanol separation of fermentation. *CHEMICAL ENGINEERING TRANSACTIONS*, 2014.

[18] W. Jin, J Zhao, and G. Liu. Design and preparation of pervaporation membranes. 2017.

[19] Alexander V. Klinov, Roald R. Akberov, Azat R. Fazlyev, and Mansur I. Farakhov. Experimental investigation and modeling through using the solution-diffusion concept of pervaporation dehydration of ethanol and isopropanol by ceramic membranes hybsi. 2017.

[20] Miroslav Kludský, Ondřej Vopička, Pavel Matějka, Štěpán Hovorka, and Karel Friess. Nafion® modified with primary amines: chemical structure, sorption properties and pervaporative separation of methanol-dimethyl carbonate mixtures. 2018.

[21] D.E. Koutsonikolas, S.P. Kaldis, Ch. Matsouka, and V.T. Zaspalis. Characterization of commercial ceramic and hybrid membranes using gas permeation and permporometry tests. 2015.

[22] Joanna Kujawa, Sophie Cerneaux, and Wojciech Kujawski. Highly hydrophobic ceramic membranes applied to the removal of volatile organic compounds in pervaporation. 2015.

[23] Qunsheng Li, Wei Zhu, Yongquan Fu, Haichuan Wang, Lun Li, and Baohua Wang. Isobaric vapor liquid equilibrium for methanol + dimethyl carbonate + 1-octyl-3-methylimidazolium tetrafluoroborate. 2012.

[24] Gongping LIU, Wang WEI, Wanqin JIN, and Nanping XU. Polymer/ceramic composite membranes and their application in pervaporation process. 2012.

[25] Hong-Xia Liu, Naixin Wang, Cui Zhao, Shulan Ji, and Jian-Rong Li. Membrane materials in the pervaporation separation of aromatic/aliphatic hydrocarbon mixtures — a review. 2018.

[26] Patricia Luis and Bart Van der Bruggen. The driving force as key element to evaluate the pervaporation performance of multicomponent mixtures. 2015.

[27] Shee-Keat Mah, Siang-Piao Chai, and Ta Yeong Wu. Dehydration of glycerin solution using pervaporation: Hybsi and polydimethylsiloxane membranes. 2014.

[28] Yee Kang Ong, Gui Min Shi, Ngoc Lieu Lea, Yu Pan Tang, Jian Zuo, Suzana P. Nunes, and Tai-Shung Chung. Recent membrane development for pervaporation processes. 2016.

[29] Roald R.Akberov, Azat R. Fazlyev, Alexander V. Klinov, Alexander V. Malygin, Mansur I. Farakhov, and Vera A. Maryakhina. Pervaporation technology for regeneration of diethylene glycol at russian complex gas treatment plants with the use of ceramic membranes hybsi. 2015.

[30] Marx S. Glycerol-free biodiesel production through transesterification: a review. 2016.

[31] H.W. Tan, A.R. Abdul Aziz, and M.K. Aroua. Glycerol production and its applications as a raw material: A review. 2013.

[32] Wai Keng Teng, Gek Cheng Ngoh, Rozita Yusoff, and Mohamed Kheireddine Aroua. A review on the performance of glycerol carbonate production via catalytic transesterification: Effects of influencing parameters. 2014.

[33] Toshinori Tsuru. Nano/subnano-tuning of porous ceramic membranes for molecular separation. 2008.

[34] Toshinori Tsuru, Akifumi Sasaki, Masakoto Kanezashi, and Tomohisa Yoshioka. Pervaporation of methanol/dimethyl carbonateusing sio_2 membranes with nano-tuned pore sizes and surface chemistry. 2010.

[35] Henk M.van Veen, Marielle D.A.Rietkerk, Donough P.Shanahan, Marc M.A.van Tuel, Robert Kreiter, Hessel L.Castricum, Johan E.ten Elshof, and Jaap F.Vente. Pushing membrane stability boundaries with hybsi® pervaporation membranes. 2011.

[36] Lei Wang, Xiaolong Han, Jiding Li, Xia Zhan, and Jian Chen. Hydrophobic nanosilica/polydimethylsiloxane membrane for dimethylcarbonate–methanol separation via pervaporation. 2011.

[37] Song Wang, Pengfei Hao, Sanxi Li, Ailing Zhang, Yinyan Guan, and Linnan Zhang. Synthesis of glycerol carbonate from glycerol and dimethyl carbonate catalyzed by calcined silicates. 2017.

[38] Yan Wang, Natalia Widjojo, Panu Sukitpaneenit, and Tai-Shung Chung. Membrane pervaporation. 2012.

[39] Wooyoung Won, Xianshe Feng, and Darren Lawless. Pervaporation with chitosan membranes: separation of dimethyl carbonate/methanol/water mixtures. 2002.

[40] Wooyoung Won, Xianshe Feng, and Darren Lawless. Separation of dimethyl carbonate/methanol/water mixtures by pervaporation using crosslinked chitosan membranes. 2003.

[41] Yang X., Ding L., Wolf M., Velterop F., J.M. Bouwneester H., Smart S., C. Diniz da Costa J., Liubinas A., Li J., Zhang J., and Duke M. Pervaporation of ammonia solution with γ-alumina supported organosilica membranes. 2016.

[42] Haoli Zhou, Lei Lv, Gongping Liu, Wanqin Jin, and Weihong Xing. Pdms/pvdf composite pervaporation membrane for the separation of dimethyl carbonate from a methanol solution. 2014.

Chapter 5

Appendices

5.1 Aspen computations

This section illustrates the activity coefficient γ and the vapour pressure P_i^0 of the two components computed by Aspen using UNIFAC method. It also shows the method used for VLE curve computation in Aspen.

5.1.1 Activity coefficient γ

The activity coefficient is detailed in Table 5.2 and Figures 5.1 to 5.3.

The gamma coefficient is estimated by an equation $ax^3 + bx^2 + cw + d$ where x is the methanol mole fraction. This equation is found using trend curve of the results obtained in Aspen.

Temperature [°C]	a	b	c	d
MeOH				
40	-0.3782	1.6337	-2.2205	1.961
50	-0.3028	1.4365	-2.0387	1.9017
60	-0.2389	1.2652	-1.877	1.8479
DMC				
40	1.3458	-0.4253	0.2522	0.9877
50	1.2578	-0.3781	0.2316	0.9887
60	1.1798	-0.3385	0.2137	0.9896

Table 5.1: Gamma equation through the curve ($ax^3 + bx^2 + cw + d$) where x is the MeOH mole fraction. The table illustrates the temperature influence as presented on Figures 5.1 to 5.3.

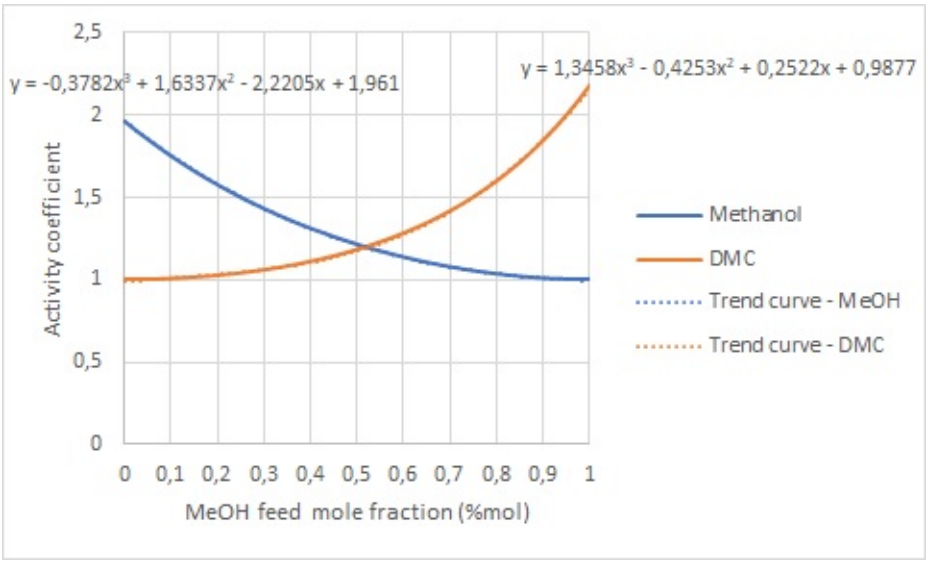

Figure 5.1: Evolution of the activity coefficient γ depending on MeOH mole fraction at 40°C.

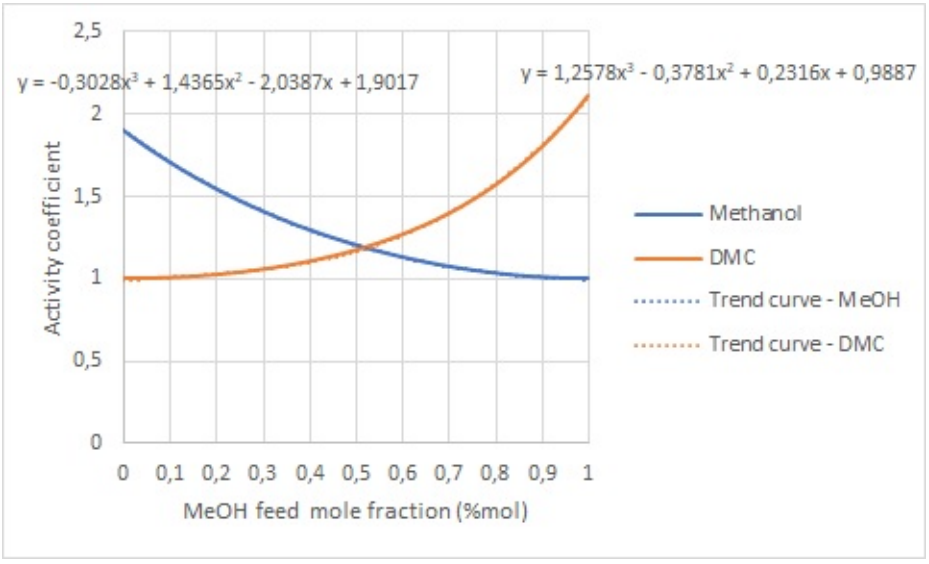

Figure 5.2: Evolution of the activity coefficient γ depending on MeOH mole fraction at 50°C.

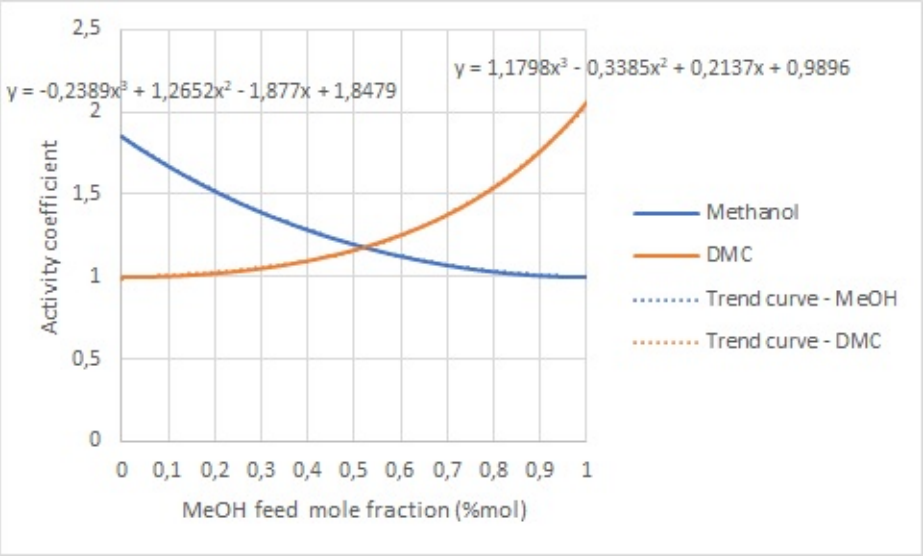

Figure 5.3: Evolution of the activity coefficient γ depending on MeOH mole fraction at 60°C.

Table 5.2: Evolution of the activity coefficient depending on the temperature and methanol mole fraction.

	40°C		50°C		60°C	
MeOH mole fraction	Liquid γ MeOH	Liquid γ DMC	Liquid γ MeOH	Liquid γ DMC	Liquid γ MeOH	Liquid γ DMC
0	1,965387	1	1,905301	1	1,850853	1
0,025	1,908597	1,000372	1,853365	1,00035	1,80319	1,000331
0,05	1,854377	1,001496	1,803647	1,001411	1,75745	1,001333
0,075	1,802612	1,003389	1,756057	1,003199	1,713563	1,003024
0,1	1,753194	1,006068	1,71051	1,005731	1,67146	1,00542
0,125	1,706021	1,009553	1,666924	1,009027	1,631078	1,008542
0,15	1,660996	1,013867	1,625223	1,013112	1,592356	1,012413
0,175	1,618028	1,019037	1,585335	1,018009	1,555235	1,017058
0,2	1,577032	1,025091	1,54719	1,023747	1,519662	1,022505
0,225	1,537927	1,032061	1,510725	1,030358	1,485584	1,028782
0,25	1,500637	1,039982	1,475877	1,037876	1,452952	1,035925
0,275	1,465091	1,048895	1,44259	1,046339	1,421719	1,04397
0,3	1,431222	1,058842	1,410808	1,055788	1,391842	1,052956
0,325	1,398966	1,069871	1,38048	1,06627	1,36328	1,062928
0,35	1,368264	1,082035	1,351559	1,077834	1,335993	1,073934
0,375	1,339062	1,095392	1,324	1,090536	1,309945	1,086027
0,4	1,311307	1,110005	1,29776	1,104436	1,285101	1,099264

	40°C		50°C		60°C	
MeOH mole fraction	Liquid γ MeOH	Liquid γ DMC	Liquid γ MeOH	Liquid γ DMC	Liquid γ MeOH	Liquid γ DMC
0,425	1,284952	1,125943	1,2728	1,1196	1,261431	1,113708
0,45	1,259952	1,143283	1,249083	1,136101	1,238904	1,129429
0,475	1,236264	1,162109	1,226577	1,154018	1,217494	1,1465
0,5	1,213852	1,182512	1,205248	1,173437	1,197174	1,165005
0,525	1,192679	1,204593	1,185069	1,194454	1,177922	1,185033
0,55	1,172714	1,228462	1,166014	1,217172	1,159717	1,206682
0,575	1,153926	1,25424	1,148059	1,241704	1,14254	1,230058
0,6	1,136291	1,282058	1,131182	1,268174	1,126375	1,25528
0,625	1,119783	1,312062	1,115366	1,29672	1,111207	1,282474
0,65	1,104383	1,344411	1,100593	1,327488	1,097024	1,311779
0,675	1,090073	1,379278	1,08685	1,360641	1,083815	1,343349
0,7	1,076837	1,416854	1,074126	1,396357	1,071573	1,377348
0,725	1,064664	1,457348	1,062412	1,43483	1,060291	1,413959
0,75	1,053543	1,500988	1,051701	1,476271	1,049966	1,453377
0,775	1,043468	1,548022	1,041989	1,52091	1,040597	1,495817
0,8	1,034434	1,598724	1,033274	1,569	1,032183	1,541512
0,825	1,02644	1,653389	1,025557	1,620812	1,024727	1,590712
0,85	1,019488	1,712341	1,018842	1,676642	1,018235	1,643691
0,875	1,01358	1,775929	1,013132	1,736807	1,012713	1,70074
0,9	1,008723	1,844528	1,008437	1,801651	1,008169	1,762172
0,925	1,004926	1,918544	1,004764	1,871538	1,004614	1,828316
0,95	1,002198	1,998407	1,002126	1,946852	1,002059	1,899521
0,975	1,000552	2,08457	1,000534	2,027997	1,000517	1,976145
1	1	2,177503	1	2,115384	1	2,058555

5.1.2 Vapour pressure P_i^0

The vapour pressure is detailed in Table 5.3.

Temperature [°C]	P^0_{MeOH} [atm]	P^0_{DMC} [atm]	P^0_{MeOH} [psia]	P^0_{DMC} [psia]
40	0,3489947	0,1489374	5,128808234	2,188776401
50	0,5480075	0,229978	8,053490149	3,379744907
60	0,8342594	0,3445436	12,26023341	5,063395097

Table 5.3: Evolution of the vapour pressure P_i^0 depending on the temperature.

5.1.3 Vapour liquid equilibrium curve

The method used in Aspen is NRTL with some variations in binary interaction coefficient shown on Table 5.4. These coefficients are coming from experimental data references [23].

Binary system	a_{mn}	a_{nm}	b_{mn}	b_{nm}	α_{mn}
DMC-MeOH	-1.7369	-0.8990	903.2140	442.4486	0.3

Table 5.4: Binary interaction coefficients for the NRTL method [23].

5.2 Distillation column example

This example is only theoretical and illustrates the use of VLE curve.

The feed content x_F equals to 0.3.

Using three stages in the distillation curve, distillate composition $y_D \simeq 0.76$ and the bottom composition $x_B \simeq 0.07$.

The separation effectively occurs. Using numerous stages nearly pure component can be produced in the bottom. However the distillate part is not optimal as the azeotropic mixture is the maximum possible distillate composition (red line). Even using infinite number of stages, the distillate composition will equal the azeotropic composition.

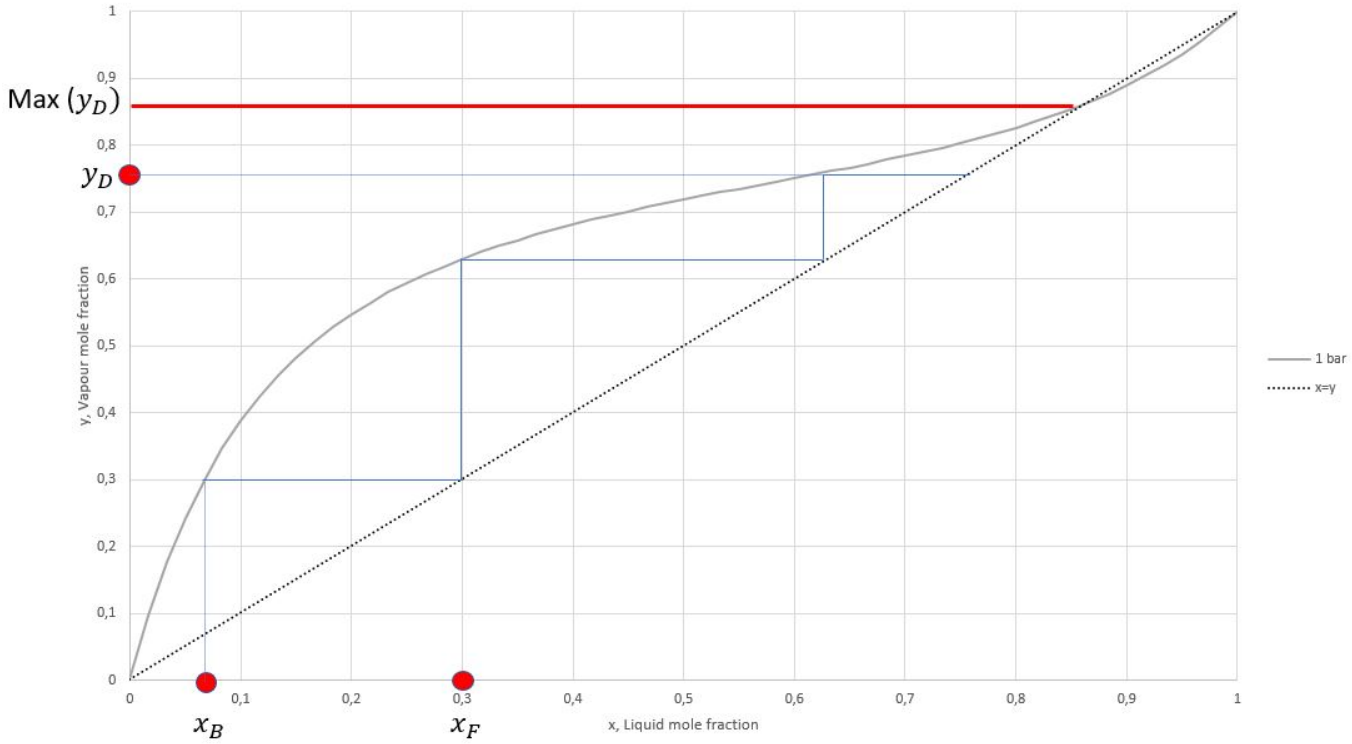

Figure 5.4: Example : usage VLE curve to analyse distillation.

This example shows the distillation limits for azeotropic mixture separation.

5.3 Figures

5.3.1 Flux evolution over time

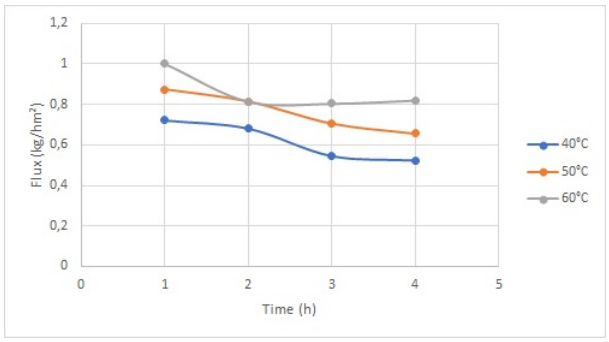

Figure 5.5: Flux evolution over time for solution of pure DMC.

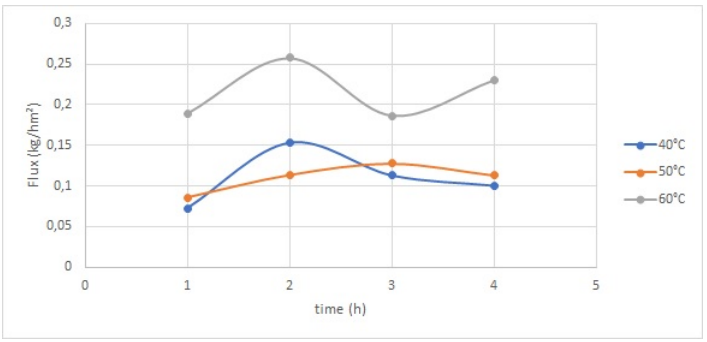

Figure 5.6: Flux evolution over time for solution of DMC(0.9) and MeOH(0.1).

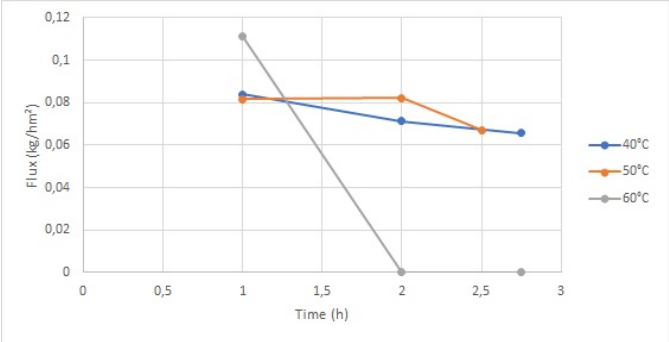

Figure 5.7: Flux evolution over time for solution of DMC(0.7) and MeOH(0.3).

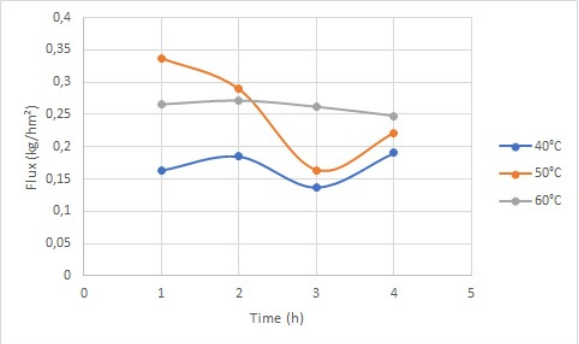

Figure 5.9: Flux evolution over time for solution of DMC(0.3) and MeOH(0.7).

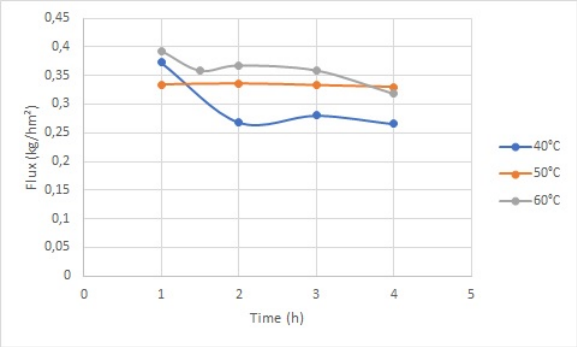

Figure 5.8: Flux evolution over time for solution of DMC(0.5) and MeOH(0.5).

5.3.2 Flux evolution over temperature

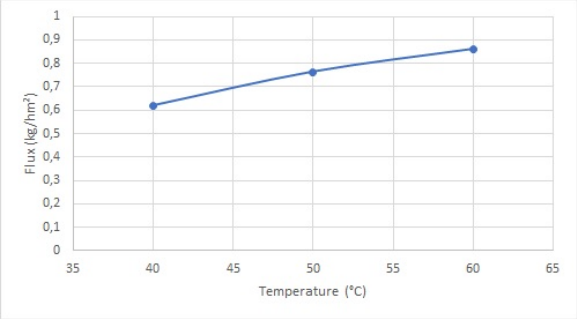

Figure 5.10: Flux evolution over temperature for solution of pure DMC.

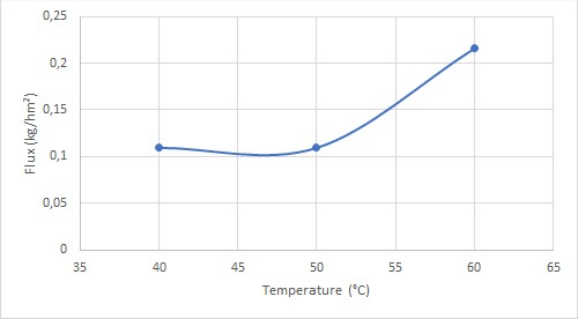

Figure 5.11: Flux evolution over temperature for solution of DMC(0.9) and MeOH(0.1).

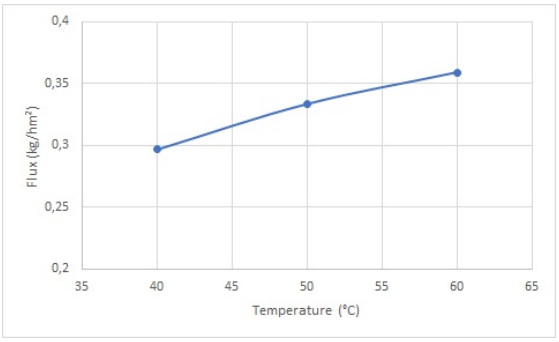

Figure 5.12: Flux evolution over temperature for solution of DMC(0.5) and MeOH(0.5).

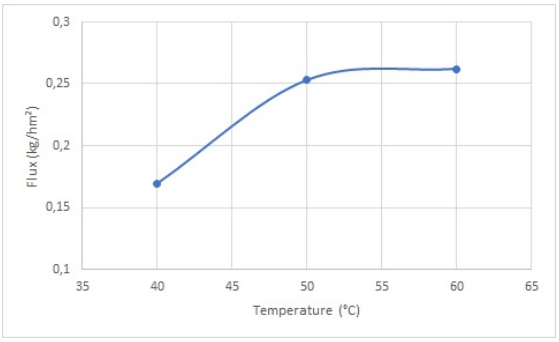

Figure 5.13: Flux evolution over temperature for solution of DMC(0.3) and MeOH(0.7).

5.3.3 Evolution of permeance through activation energy

Figure 5.14 shows the evolution of temperature using equation 2.12 including activation energy and pre-exponential factor found in section 3.2.4.

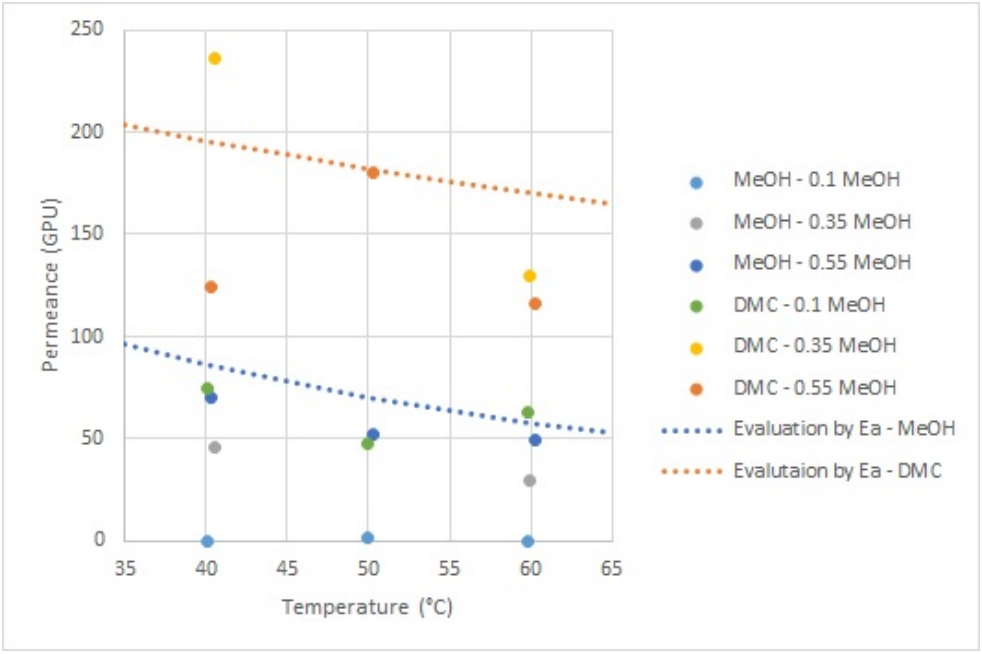

Figure 5.14: Evolution of the permeance depending on the activation energy. Dotted lines are the evaluation using E_a. Points are the experiments data depending on feed content (MeOH mass fraction).

Rue Archimède, 1 bte L6.11.01, 1348 Louvain-la-Neuve, Belgium **www.uclouvain.be/epl**